Swiss Journal of Palaeontology

RESEARCH ARTICLE

Open Access

Geochemical investigation of the mixed Máriahalom vertebrate fauna at the Paleogene–Neogene boundary in the Central Paratethys: environmental conditions and age constrain

László Kocsis[1*], Márton Rabi[2,3], Alex Ulianov[4], Anna Cipriani[5,6], Izabella M. Farkas[7] and Gábor Botfalvai[8,9,10]

Abstract

The fossil vertebrate fauna of Máriahalom contains remains from a wide range of ecologies including terrestrial and aquatic mammals, crocodiles, sharks, and rays among others. All these were found mixed in mollusc-rich, shallow water, coastal deposits. The aim of the study is to trace the origin of the fossils using their rare earth element (REE) content and their respective ecology with stable oxygen isotopic compositions. In addition, marine vertebrates and calcareous marine fossils were analysed for their Sr isotope composition to provide a new age estimate for the locality. The REE content and their distribution in the fossils indicate similar early diagenetic environments and possible contemporaneous fossilization for the entire vertebrate assemblage. Reworked fossils of significantly different age can be excluded. The enamel/enameloid-derived phosphate oxygen isotope composition of selected fossil taxa fit well with previously inferred habitats that include marine, brackish, and terrestrial environments. Notably, the stem-pinniped *Potamotherium valletoni* is best interpreted as freshwater dweller instead of marine, consistent with the sedimentology of other occurrences. Our novel $^{87}Sr/^{86}Sr$ data suggest an Aquitanian age (21.4 ± 0.5 Ma) for the Máriahalom site that is younger than the previously proposed Late Oligocene age based on biostratigraphy (MP28–30 European Mammal Paleogene Reference Levels). An Aquitanian age raises the possibility that the index fossil taxon, the anthracothere mammal *Microbunodon minimum*, may have vanished earlier in Western Europe than in the Central Paratethys region.

Keywords Bioapatite, Stable isotopes, Rare earth element taphonomy, Strontium isotope stratigraphy, Mammal biostratigraphy

Handling editor: Thomas Martin.

*Correspondence:
László Kocsis
laszlo.kocsis@unil.ch
[1] Institute of Earth Surface Dynamics, Faculty of Geosciences and Environment, University of Lausanne, Lausanne, Switzerland
[2] Institute of Geosciences, University of Tübingen, Hölderlinstraße 12, 72074 Tübingen, Germany
[3] Central Natural Science Collections, Martin-Luther University Halle-Wittenberg, 06108 Halle (Saale), Germany
[4] Institute of Earth Sciences, Faculty of Geosciences and Environment, University of Lausanne, Lausanne, Switzerland
[5] Dipartimento Di Scienze Chimiche E Geologiche, Universita Di Modena E Reggio Emilia, Modena, Italy
[6] Lamont-Doherty Earth Observatory, Columbia University, Palisades, NY, USA
[7] Laboratories MOL, MOL Plc, Szent István Street 14, Budapest H-1039, Hungary
[8] Institute of Geography and Earth Sciences, Department of Paleontology, ELTE Eötvös Loránd University, Budapest, Hungary
[9] ELKH-MTM-ELTE Research Group for Paleontology, Budapest, Hungary
[10] Department of Palaeontology and Geology, Hungarian Natural History Museum, Budapest, Hungary

Introduction

The fossil locality of Máriahalom (Mány-Zsambék Basin, northern Hungary) yielded a rich mollusc assemblage as well as a mixed vertebrate fauna of marine, freshwater, and terrestrial origins, deposited in a shallow marine coastal setting influenced by tide and wave actions of the Central Paratethys (Fig. 1) (Báldi, 1967; Báldi & Cságoly, 1975; Sztanó et al., 1998; Rabi & Botfalvai, 2008; Szabó et al., 2017; Rabi et al., 2018). The age of the beds is considered Egerian (Late Chattian—Early Aquitanian), but the exact boundary of the Paleogene and Neogene cannot be defined in the absence of the index fossil foraminifer for the Aquitanian (*Paragloborotalia kugleri*) in the Central Paratethys (e.g. Báldi et al., 1999; Piller et al., 2007). The vertebrate fauna contains elements (e.g. the anthracothere *Microbunodon minimum*) that would rather support Latest Oligocene age (Rabi et al., 2018); however, the mixed nature of the fauna cannot discard the possibility that some of these remains were reworked from older beds.

In this study, we conducted rare earth element (REE), as well as oxygen and strontium isotope analyses to better constrain the depositional history, palaeoecology, and the age of the fossil fauna.

Geochemical proxies

Taphonomical and sedimentological investigations of the vertebrate fossils (bones and teeth) are extremely useful to determine the depositional histories and environmental settings of vertebrate assemblages (e.g. Behrensmeyer, 1991; Botfalvai et al., 2015, 2017). Besides these traditional investigations, geochemical analyses of the fossils are also commonly applied (e.g. Anderson et al., 2007; Kocsis et al., 2020; Trueman, 1999, 2007). Bone fossilization can be viewed as the process of recrystallization of biogenic apatite to carbonate fluorapatite (francolite), and during this process many trace elements can be incorporated into the fossil bones (Keenan & Engel, 2017; Trueman & Tuross, 2002). Apatite has a strong affinity for the rare earth elements (REE), which are only sparsely present in body fluids, but soil and pore waters often contain somewhat larger concentrations of these elements (Trueman, 1999, 2007). When the bones are exposed postmortem to these fluids, the concentrations of REEs increase dramatically in a relatively short time during the fossilization; hence, the buried bones record fingerprints or signatures diagnostic of the burial environment (e.g. Trueman & Tuross, 2002; Trueman et al., 2006). Based on these listed features, the bones that recrystallized in different depositional settings inherit different trace element (TE) compositions, and thus, variations in the TE signatures within a bonebed can be used to infer post-depositional transport and mixing of vertebrate assemblages and to unravel the accumulation histories of such mixed faunas (Botfalvai et al., 2022; Kocsis et al., 2020, 2021; Trueman et al., 2004, 2006). Therefore, the fossil-rich, ecologically mixed vertebrate accumulation of the Máriahalom is an ideal site to test the remains with geochemical taphonomy. The incorporation of REEs into the bioapatite structure depends on the crystal size and original organic content of the investigated material. The uptake can be also viewed as a diffusive process from the external REE source of the pore fluid towards the internal parts of bones and teeth, and concentration gradients along specimens are often observed (e.g. Herwartz et al., 2013; Kohn & Moses, 2012; Millard & Hedge, 1996; Schroeter et al., 2022; Trueman et al., 2011). On the other hand, protracted REE uptake with time was also reported (Herwartz et al., 2011; Kocsis et al., 2010; Kowal-Linka et al., 2013) that may hinder palaeoenvironmental interpretation of the early diagenetic conditions.

Although the REE elements are almost entirely incorporated into the bioapatite [$\sim Ca_5(PO_4, CO_3)_3(OH, F, CO_3)$] during diagenesis, stable isotope compositions of the major anions ($\delta^{13}C_{CO3}$, $\delta^{18}O_{CO3}$, $\delta^{18}O_{PO4}$) of fossil teeth and bones can still reflect ecological conditions and habitats of the vertebrates and, therefore are widely used in palaeoenvironmental and palaeoclimate studies (e.g. Kohn & Cerling, 2002 and reference therein). Oxygen isotope composition of ectotherm aquatic organisms can be linked to ambient temperature and the isotopic composition of environmental water (e.g. Kolodny et al., 1983; Lécuyer et al., 2013). In case of terrestrial mammals, carbon isotopic composition of their skeletal remains can reflect diet, while the oxygen isotope composition could be related to their body water via which the local climate can be traced (e.g. Bryant & Froelich, 1995; Fricke et al., 1998; Kocsis et al., 2014; Kohn & Cerling, 2002; Longinelli, 1984; Makarewicz & Pederzani, 2017; Tütken et al., 2006, 2013).

Strontium isotope ratios ($^{87}Sr/^{86}Sr$) of well-preserved marine calcareous and phosphatic fossils are often used to date marine sections via comparing the obtained values with the global Sr isotope reference curve (McArthur et al., 2001, 2020). The basis of this method lies in the fact that Sr has a long residence time in seawater ($> 10^6$ yrs), longer than that of oceanic turnover (10^3 yrs), which results in an overall unique Sr isotope composition for the open ocean (e.g. Burke et al., 1982; DePaolo & Ingram, 1985; Veizer, 1989). However, on a longer time scale, the $^{87}Sr/^{86}Sr$ of the ocean varied depending on the proportion of the Sr input into the ocean (i.e. higher ratios—continental crustal source, lower ratios—mantle-derived Sr). When marine organisms secret their shells or skeleton, they incorporate Sr into their biominerals without fractionation; hence, their remains can be used

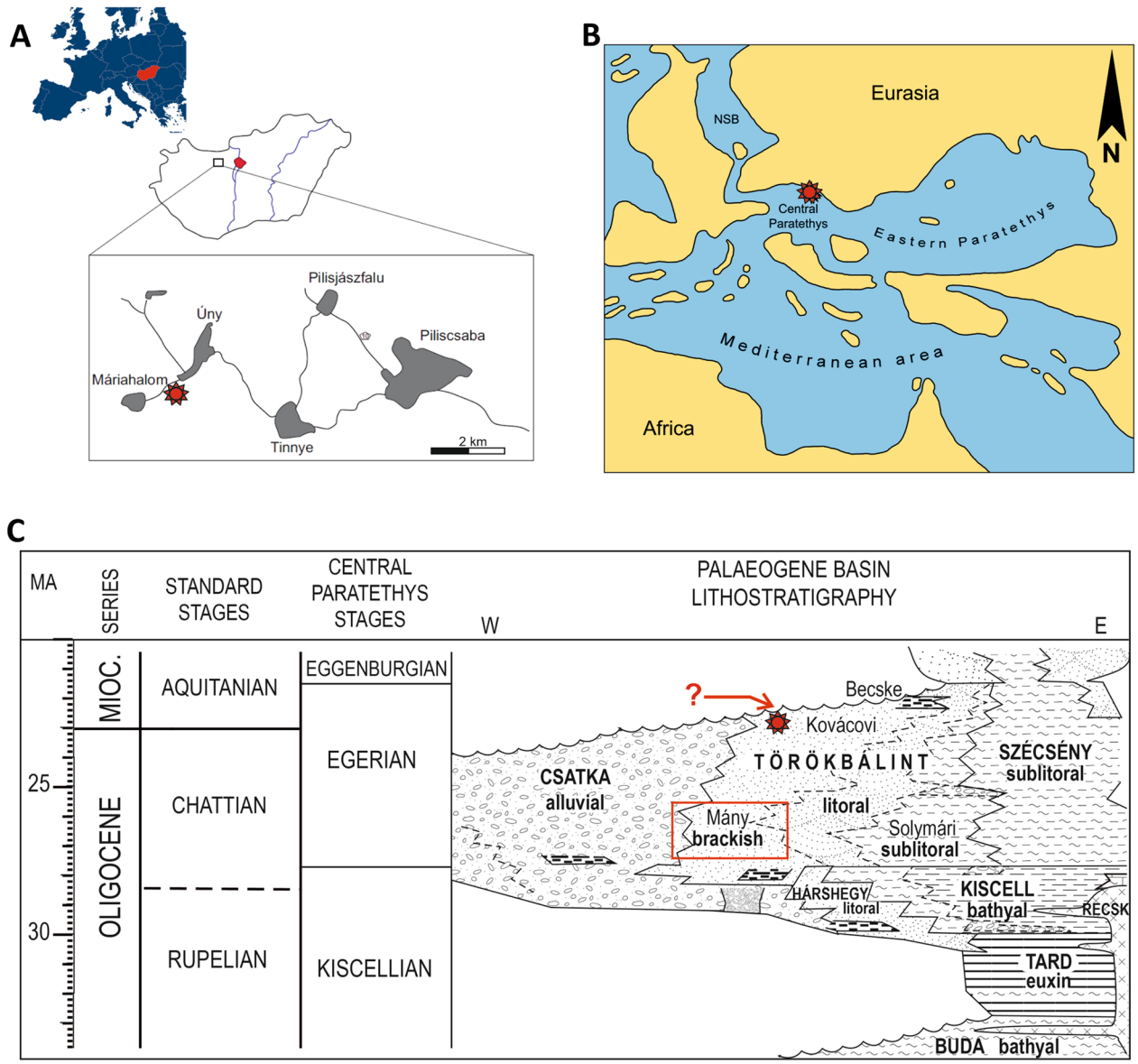

Fig. 1 Geography and geology of the Máriahalom site. **A** Locality map; **B** Palaeogeographical map of the Paratethys region during the Oligocene–Miocene interval (modified after Harzhauser & Piller, 2007). The Máriahalom site is indicated by the red symbol; **C** Stratigraphic units and their depositional environments mentioned in this study (published in Szabó et al., 2017) Note: top of the Törökbálint Formation (including the Mány Member) can be reassessed based on the $^{87}Sr/^{86}Sr$ data published in this study (see below)

to trace open ocean origin and the age of their embedding sediment.

Geological background

The Paratethys evolved as an epicontinental sea initially covering the present area between the Western Alps and Lake Aral. It was isolated from the Tethys Ocean during the Late Eocene–Early Oligocene due to the Alpine orogeny related to Africa's northward movement and counterclockwise rotation resulting in the subduction of the European plate (Popov et al., 2004 and references therein). This caused the final disintegration of the Western Tethys Ocean and created the Mediterranean Sea at the western end of the Tethys, while the Paratethys Sea arose north of this tectonic belt. The connection between the two basins was restricted in certain times, which significantly limited faunal exchange leading to different fauna compositions.

The Paratethys can be separated into three palaeogeographic and geotectonic units namely

Western- Central and Eastern Paratethys each recording a different environmental history (Piller et al., 2007). The Eastern Paratethys is the largest part and includes the present-day area of Black Sea, Caspian Sea, and Lake Aral basins, while the Western part comprises the Alpine Foreland Basins of France, Switzerland, and part of Germany and Upper Austria (Piller et al., 2007; Popov et al., 2004; and references therein). The Central Paratethys is situated between the western and eastern realms, and it consists of the Eastern Alpine—Pannon–Carpathian Basins (Fig. 1b). The former area of Máriahalom was situated in the Central Paratethys during the Late Paleogene–Early Neogene period (Piller et al., 2007; Popov et al., 2004; Fig. 1b).

Isolation and reopening of oceanic gateways to the Paratethys occurred repeatedly, allowing the development of distinct palaeobiological provinces characterized by endemic evolution and difficulties in global stratigraphic correlations.

Máriahalom is in the Transdanubia Range of Hungary, which is part of the Hungarian Paleogene Basin (HPB). The HPB was filled up with sediments from the Middle Eocene to Early Miocene interval forming a single extensive sedimentary cycle. During the Eocene and the earliest Oligocene, the transgression gradually progressed from SW to NE, characterized by intensive faunal exchange with the Mediterranean realm. During the Early Oligocene, large parts of the Transdanubian Range was uplifted, and denudation removed the top part of the Eocene sections and the entire Lower Oligocene deposits (Báldi, 1983; Kázmér et al., 2003; Telegdi-Roth, 1927), while restricted, anoxic shales (Tard Clay Formation) were deposited in the eastern (Fig. 1c), deeper part of the HPB basin. In this time, the seaway towards the Mediterranean and also the northern connection to the global marine system had been closed due to the Alpine-Carpathian orogeny and eustatic sea level drop (Miller et al., 2020).

From the later part of the Kiscellian (Late Rupelian; Tari et al., 1993), transgression allowed re-establishing marine connections towards the Mediterranean. Thereafter, a new shallow marine basin is formed with lagoonal and freshwater deposition towards the margins (Hárshegy Sandstone Formation) (Szederkényi et al., 2012; Sztanó et al., 1998). Due to gradual subsidence of the basin, shallow bathyal deposition prevailed, and the Kiscell Clay Formation accumulated (Báldi, 1983).

During the Late Oligocene–Early Miocene (Egerian stage), sediment input from the west increased and long-term normal regression resulted in the interfingering alluvial Csatka and the marginal marine to neritic Törökbálint formations (Korpás, 1981; Nagymarosy & Gyalog, 1997; Sztanó et al., 1998). The Törökbálint Formation represents deposits from brackish to normal marine conditions of which the brackish part is separated as the Mány Member (Korpás, 1981; Nagymarosy, 2012; see Fig. 1c). The Oligocene/Miocene transition is characterized by a regression trend (e.g. Széchényi Schlier Formation) and in many cases the Early Miocene denudation also affected the deeper Oligocene beds, resulting in reduced thickness of Paleogene strata.

Position and depositional environment of the Máriahalom site

The Máriahalom site is an abandoned sand-pit located 47 km north-west from Budapest (Hungary), between the villages of Úny and Máriahalom, within the Mány-Zsámbék Basin (part of the Transdanubian Range) of the HPB (Fig. 1a). The exposed section in the quarry is predominantly characterized by highly matured quartz sand (beach), sandy clay, and interbedded sandstone bodies. The exposed sediments are characterized by a predominantly brackish mollusc fauna (*Potamides-Pirenella* community, see detailed in Báldi 1967 and Báldi & Cságoly, 1975) that represents a transition between alluvial and normal marine conditions. It is interpreted as a product of lagoonal environments (Báldi, 1967; Nagymarosy & Gyalog, 1997; Nagymarosy, 2012), which was possibly connected to a delta plain environment (Szabó et al., 2017; Sztanó et al., 1998).

The vertebrate fossils studied here were found isolated and they have been collected from 2 to 5 m wide, 1–1.5-m–thick coquina-like accumulations situated in the uppermost part of the exposed section at the northeast wall of the quarry. This coquina-like, bonebed accumulation is composed almost entirely of transported, abraded, and mechanically sorted mollusc shells, where the amount of the siliciclastic sediments is subordinate compared to the fragmented bioclasts. In the bonebed, remains of shallow marine (sharks, rays, and bony fishes), freshwater (turtles, crocodiles, and mammals), and terrestrial (mammals) vertebrates are found together probably as a result of wash-in of skeletal elements from the shore into the marine depositional area due to wave action (Rabi et al., 2018; Szabó et al., 2017).

Based on the above explained sedimentological, taphonomical, and palaeontological evidence, the depositional environment is characterized by high energy conditions with tidal influence (e.g. Szabó et al., 2017). The bone-rich bed probably represents a channel fill deposit, which has been formed on a delta plain embayment or a tidal flat characterized by intense tidal influence (Szabó et al., 2017). In summary, the examined vertebrate assemblage was deposited in a transitional environment between the

normal marine and terrestrial habitats, which was characterized by relatively low salinity and high energy conditions (Rabi et al., 2018; Szabó et al., 2017).

Age of the Máriahalom fauna

The above-mentioned sedimentological and palaeontological data indicate that the examined section at the Máriahalom site corresponds to the Mány Member of the Törökbálint Formation (Báldi, 1967; Nagymarosy & Gyalog, 1997; Nagymarosy, 2012; Szabó et al., 2017). Deposits of the Mány Member belong to the transitional zone between the marginal marine to neritic Törökbálint Sandstone Formation and the alluvial (deltaic) system of the Csatka Formation (Fig. 1c). The 300–500-m-thick Mány Member belongs to the Egerian Paratethys stage based on mollusc biostratigraphy derived from more than 50 boreholes (Báldi et al., 1999; Báldi & Cságoly, 1975; Nagymarosy & Gyalog, 1997; Piller et al., 2007). The Egerian chronostratigraphic stage is a local stage developed for the Central Paratethys Basin. The age of the basal part of the Egerian stage corresponds to the upper Chattian, while the upper part can be correlated with the lower Miocene (Aquitanian or Aquitanian / Burdigalian boundary) based on biostratigraphy and preliminary Sr isotope stratigraphy data (Báldi et al., 1999; Less et al., 2015; Piller et al., 2007; Rögl, 1998). However, the Oligocene/Miocene boundary is difficult to detect in the Egerian stage due to the absence of Aquitanian marine index fossils in the Central Paratethys region such as the *Paragloborotalia kugleri* (e.g. Báldi et al., 1999; Piller et al., 2007).

Despite the chronostratigraphic uncertainties of the Egerian stage mentioned above, the exposed section of the Mány Member at the Máriahalom site was interpreted and referred to as an Oligocene succession (Báldi & Cságoly, 1975; Rabi & Botfalvai, 2008; Rabi et al., 2018; Szabó et al., 2017) on the basis of the presumed stratigraphic position of the brackish mollusc fauna in

Table 1 Vertebrate faunal list of the Máriahalom site

Taxon		Material	References
Chondrichthyes	*Squatina* sp.	Teeth	Szabó et al. (2017)
	Araloselachus cuspidatus	Teeth	
	Carcharias cf. *acutissima*	Teeth	
	Carcharias gustrowensis	Teeth	
	Bakonybatrachus fedori	Teeth	
	Carcharoides catticus	Teeth	
	Cosmopolitodus sp.	Teeth	
	Carcharhinus sp.	Teeth and vertebrae	
	Aetomylaeus sp.	Teeth	
	Myliobatis sp.	Teeth	
	Rhinoptera cf. *schultzi*	Teeth	
	Rhinoptera cf. *studeri*	Teeth	
Osteichthyes	aff. *Morone* sp.	Otolith	
	Sparidae indet	Premaxillae and dentaries	
	Sciaena sp.	Otoliths	
	Aglyptorhynchus sp.	Rostras, vertebra	
	Trichiuridae indet	Teeth	
Chelonia	Trionychoidea indet	Plate fragments	Rabi and Botfalvai (2008)
	Testudinoidea indet	Plate fragments	
Squamata	Squamata indet	Vertebrae	
Crocodilia	Crocodylia indet. (cf. *Diplocynodon* sp.)	Teeth, bones	
Aves	(?) Anseriformes indet	Bones	
Sirenia	Sirenia indet	Ribs, skull fragment	
Artiodactyla	*Microbunodon minimum*	Teeth, jaw fragment	
Carnivora	*Potamotherium valletoni*	Teeth, tibia	Rabi et al. (2018)
	Amphictis sp. or *Franconictis* sp.	Teeth	
	Mustelidae indet	Teeth	
	Pachycynodon boriei	Teeth	

the basin (Báldi & Cságoly, 1975; Piller et al., 2007), and the fossil terrestrial mammal *Microbunodon minimum* (Cuvier, 1822) (Rabi & Botfalvai, 2008; Rabi et al., 2018). However, the new $^{87}Sr/^{86}Sr$ data reported in this study suggest an earliest Miocene age instead (see below).

Fauna overview

The invertebrate and vertebrate taxa from Máriahalom include normal marine, freshwater, and terrestrial elements (Table 1). All vertebrate remains consist of isolated teeth and mostly fragmentary bones.

The remarkably abundant and well-preserved mollusc fauna of Máriahalom has been classified as a *Potamides-Pirenella* community, possibly reflecting a brackish lagoon environment, although less common, normal marine taxa (e.g. *Glycymeris latiradiata*, *Mytilus aquitanicus*) are also present (Báldi & Cságoly, 1975; Janssen, 1982).

The fish assemblage represents a marine subtropical-tropical littoral community (Szabó et al., 2017). Based on the isolated elasmobranch and bony fish remains 8 sharks, 4 rays, and 7 teleosts were identified. The fauna is dominated by piscivorous taxa (odontaspids and carcharhinids); however, large, macropredatory sharks (e.g. *Otodus*) also occurred.

The reptilian material includes remains of turtles (trionychid and testudinoid), crocodilians, and squamata (Rabi & Botfalvai, 2008). Regarding mammals, despite the small sample size of the carnivoran remains, four separate taxa could be identified including the semi-aquatic basal mustelid *Potamotherium valletoni*, the small-sized, terrestrial basal mustelidean *Amphictis* sp. or *Franconictis* sp., another indeterminate basal mustelidean, and the medium-sized, terrestrial basal ursoid *Pachycynodon boriei* (Rabi et al., 2018). Other mammals such as *Microbunodon minimum*, sirenians, and medium-size herbivore mammals were also discovered (Rabi & Botfalvai, 2008).

Material and methods

Trace element analyses

From 2- to 4-mm-sized chips of bones and teeth were taken from 16 selected samples including remains of terrestrial, freshwater, and marine animals. The coverage of the different habitats within the mixed vertebrate fauna was important to check whether different taphonomic signatures could be detected from possible previous deposits. The chosen specimens, and the type and parts of the bones and teeth, are listed and illustrated in Additional file 3: Table S1 and Additional file 1: Figure S1. The specimens were embedded in epoxy resin and then polished for Laser Ablation Inductively Coupled Plasma Mass Spectrometry (LA-ICP-MS). The ablation was carried out in a Helium atmosphere using spot sizes of 100 µm in diameter. Each specimen was ablated between 1 and 4 times. Trace element contents were determined using an Element XR single collector sector field ICP-MS interfaced to a RESOlution SE 193 nm excimer ablation system equipped with an S155 two-volume ablation cell. The analyses were carried out at the University of Lausanne, Switzerland. Our study focused on the rare earth elements; however, other trace elements were analysed too (see Additional file 3: Table S1). Standard reference material of NIST612 was used for external standardization, and as an internal standard ^{42}Ca was analysed, and CaO values of 54 and 50 wt.% were used for enameloid/enamel and for dentine and bone, respectively (e.g. Kocsis et al., 2021). The analytical reproducibility was generally better than ± 5% SE. The obtained data allow relative comparison between samples and sites using element ratios or PAAS (Post Archean Australian Shale)-normalized REE patterns. The REEs are subdivided into light (LREE: La, Pr, Ce, Nd), middle (MREE: Eu, Gd, Tb, Dy), and heavy rare earth element (HREE: Er, Tm, Yb, Lu) groups. MREE* is defined by the average of LREE and HREE.

Stable isotope analyses

To test palaeoenvironmental conditions at the Máriahalom site, vertebrate taxa characterized by different ecology were chosen for stable isotope analyses. Four shark teeth (*Araloselachus cuspidatus* VER 2016.2743., *Carcharoides catticus* VER 2016.2741., and two odontaspids VER 2016.2744.), a cf. *Diplocynodon* sp. crocodilian tooth (VER 2016.3561.), a seacow rib (VER 2016.3562.), a carnivore (*Potamotherium valletoni* VER 2016.3565.), and two herbivore mammal teeth (*Microbunodon minimum*, VER 2016.3563. and VER 2016.3564.) were prepared for the measurements. The samples were cleaned in an ultrasonic bath; then enameloid, enamel, and in some cases, dentine and bone, were sampled with a microdrill. The powders were briefly leached in acetic acid buffered by Ca Acetate to pH 4.5 to remove any exogenous carbonate. A subset of the samples was prepared via separating the PO_4^{3-} ion that precipitated as Ag_3PO_4 (e.g. Dettman et al., 2001; O'Neil et al., 1994) and then analysed for $\delta^{18}O$ with high-temperature conversion elemental analyser (TC/EA, see Vennemann et al., 2002). Each sample ran as triplicates and the results were corrected to in-house Ag_3PO_4 standards that had better than ± 0.3 ‰ standard deviation. All these data are expressed relative to VSMOW (Vienna Standard Mean Ocean Water). NIST SRM 120c phosphorite standard material was run parallel with the samples and yielded $\delta^{18}O$ values of 21.5 ± 0.2 ‰ ($n = 4$). Few calcareous shells were also measured for

Table 2 Strontium isotope ratios, related ages, and in case of the calcareous fossils X-ray diffraction, stable isotope composition, and minor and trace element ratio data. Abbreviations: arg - aragonite, cal - calcite, q - quartz.

Sample		$^{87}Sr/^{86}Sr$	2SE *10^{-6}	SIS Age			Mineralogy (%)			$\delta^{13}C$ ‰, VPDB	1SD	$\delta^{18}O$ ‰, VPDB	1SD	Yield % ($CaCO_3$)	Mg/Ca	Sr/Ca	Fe/Ca	Mn/Ca
				–	My	+	q	cal	arg						mmol/mol			
Aragonite																		
Glycymeris—bivalve	**G1**	0.708358	5	0.3	**21.3**	0.3	–	8	92	1.24	0.06	−1.97	0.08	96	8.31	1.40	0.49	0.04
Nerineidae-gastropoda	**N1**	0.708355	5	0.3	**21.4**	0.4	–	1	99	−0.61	0.04	−2.83	0.09	102	5.78	1.34	1.16	0.07
Calcite																		
Ostrea—bivalve	O2	0.708189	5	0.4	24.2	0.4	0.5	98.5	1	−2.86	0.06	−4.89	0.07	101	11.15	0.63	0.82	0.20
Apatite																		
Shark tooth enameloid	**SE1**	0.708338	4	0.3	**21.6**	0.4												
Shark tooth enameloid	SE3	0.708406	4	0.3	20.6	0.3												
Shark tooth root	SR2	0.708898	3	0.9	9.6	0.8												

It is noted that the calcareous fossils largely preserved their original mineralogy. The Sr isotope ages are derived from McArthur et al. (2020), and the upper and lower age limits were calculated based on the 95% confidence limit of the curve and the error related to the Sr isotope analyses. As the internal reproducibility of the individual analyses is lower than that of the external one derived from repeated analyses of the NIST SRM 987 standard (18 ppm, 2SD, $n = 14$); hence, this later was used to calculate error on the ages.

It is noted that the suggested age for the Máriahalom site derives from the specimens G1, N1, and SE1 (21.4 ± 0.5 Ma). The name of these specimens and their SIS ages are marked bold.

carbon and oxygen isotope compositions as a part of a screening method before SIS dating (see below). The analyses were done on a Gasbench II coupled to a Finnigan MAT Delta Plus XL mass spectrometer via reacting the samples with phosphoric acid (Spötl & Vennemann, 2003). The analytical precision for this method was better than ± 0.1‰ standard deviation. The stable isotope values are expressed in the δ-notation in case of the $\delta^{18}O_{PO4}$ relative to VSMOW, while in the cases of the $\delta^{18}O_{CO3}$ and $\delta^{13}C$ values relative to VPDB (Vienna Pee Dee Belemnite, Additional file 4: Table S2). All these measurements were carried out at the stable isotope laboratory of Institute of Earth Surface Dynamics, University of Lausanne, Switzerland.

Strontium isotope ratios and related analyses

Different biominerals (aragonite, calcite, bioapatite) with different structures (shark tooth dentine vs enameloid) were selected for Sr isotope analyses. Bioapatite is represented by two shark tooth enameloid and one root, aragonitic shells by a *Glycymeris* bivalve and a Nerineidae gastropod, and lastly calcite shell by an *Ostrea* bivalve (Table 2). Some of the samples were further screened with different methods and the results are summarized in Table 2. First the samples were powdered, and prior to strontium isotope preparations, the three calcareous specimens were tested for mineralogical composition by X-ray powder diffraction using a Bruker D8 Advance powder diffractometer with parallel beam, 2θ-θ geometry equipped with LynxEye© 1D detector. The measuring parameters were step-scanning at 0.01° 2θ intervals and counting time of 35.4 s (0.2). CuKα radiation at 40 kV and 40 mA was used. The measurement range was 5–70° 2θ. The identification of minerals was achieved using the Diffrac EVA software by comparison of the X-ray diffraction pattern from the sample with the International Centre for Diffraction Data PDF-2, release 2009 database. The quantitative data were obtained using TOPAS software providing us a standardless quantitative analysis (based on Rietveld method). The measurements were made at MOL Laboratories in Budapest, Hungary. The obtained diffractograms are provided in Additional file 2: Figure S2 document. Sub-samples were also run for stable isotope analyses as described above (see also Table 2).

The samples were then further handled at the Department of Chemical and Geological Sciences of the University of Modena and Reggio Emilia (UNIMORE), Italy. They were dissolved, and sub-solutions of the calcareous samples were measured for concentration of Mg, Sr, Mn, and Fe on a Perkin Elmer Optima 4200 DV ICP-OES. The supernatant was diluted to 4% w/w HNO_3 for the analyses, while an aliquot of the sample was further diluted to measure Ca concentration as well. The ICP-OES was externally calibrated with multielement calibration standards in the concentration range from 1 ppb to 10 ppm for all the elements. Precisions were typically better than 5% RSD (relative standard deviation) for Ca, Mg, Sr, and Fe and better than 20% for Mn. The data are expressed in ratios relative to Ca in mmol/mol (Table 2). The rest of the solution is then processed using standard cation exchange to separate strontium with Eichrom Sr-spec resin filled columns. The Sr isotopic ratios were analysed via a double-focusing MC-ICPMS with a forward Nier–Johnson geometry (Thermo Fisher Scientific, NeptuneTM). All the data were adjusted to an $^{86}Sr/^{88}Sr$ value of 0.1194 as fractionation correction. The samples were run together with several NIST SRM 987 standards, and their 2 standard deviations were used to correct for instrumental bias to a value of 0.710248 (McArthur et al., 2001). Repeated analyses of the NIST SRM 987 yielded external reproducibility (2SD) of 18 ppm ($n=14$). The $^{87}Sr/^{86}Sr$ ratios of the samples then were compared to the look-up tables of McArthur et al. (2020), which is tied to the Geological Time Scale 2020 (Gradstein et al., 2020), and were used to derive numerical ages. The errors related to the analyses (internal and external reproducibilities) and the error associated with the Sr evolution curve (i.e. 95% confidence interval) were considered in the age calculations.

Results

Rare earth element composition

Sixteen vertebrate specimens were analysed with multiple in situ laser spots ($n=41$). The data were scrutinized and then averaged relating to the specimens, their different types of material (e.g. enamel vs dentine), and their PAAS-normalized REE patterns, resulting in 29 final data points (Fig. 2 and Additional file 3: Table S1). The total REE contents range from 1.3 to 10,045 ppm (mean = 1997 ppm; median = 1062 ppm). The lowest value is from a mammal tooth dentine (M16), while the highest REE content came from a crocodile scute (M12). Generally, the denser and higher mineralized material such as tooth enameloid/enamel yielded low REE concentration, and/or the more internal part of bone and dentine within the specimens. Another observation is that the lighter coloured bones show relatively higher mean REE content than the darker ones (e.g. crocodile scute M12 and M11; turtle plates M8, M9, and M7) (Additional file 1: Figure S1). In terms of taxa, the overall shark tooth data (M1-M3) have a lower REE content compared to bones and teeth of other vertebrates; otherwise, there is no significant difference in REE content between the terrestrial, freshwater, and marine remains.

The PAAS-normalized REE patterns show two endmembers, a middle REE-enriched pattern and a

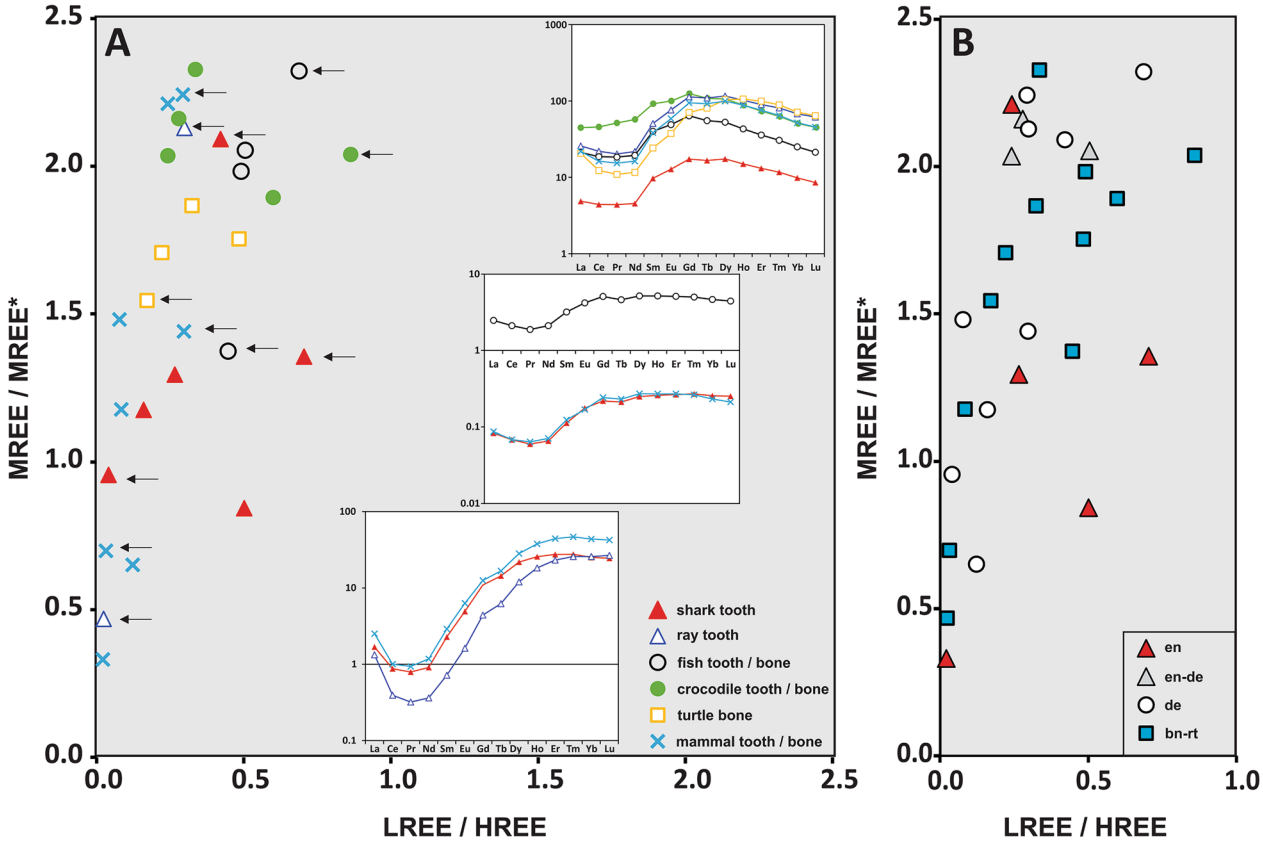

Fig. 2 PAAS-normalized REE element ratios and selected REE element patterns of the Máriahalom vertebrates. **A** The plot is based on taxonomy. **B** The plot is based on the analysed material (en: enamel/enameloid, en-de: enamel–dentine mixture, de: dentine: bn-rt: bone or root). The LREE, MREE, HREE represent the average of the light (La, Pr, Ce, Nd), middle (Eu, Gd, Tb, Dy), and heavy (Er, Tm, Yb, Lu) REE. MREE* represents the average of the LHREE and HREE. Note that the data vary between an MREE-enriched and a LREE-depleted endmembers. Importantly, both types of patterns can exist in the very same fossils. The first rather reflects environmental REE variation, while the second relates to REE uptake mechanism (see text). Horizontal arrows mark data points with displayed REE patterns on the right. The REE patterns are plotted in a logarithmic scale; it is noted that some of the specimens are more enriched, while others are depleted in REE

LREE-depleted ones (Fig. 2). The latter group has in general lower REE content. The spread of the data on an MREE/MREE* versus LREE/HREE diagram further emphasizes the REE distribution in the samples between these two endmembers. In addition, the data have larger variation along the MREE compared to LREE/HREE (Fig. 2). It must be pointed out that there are no taxonomic differences related to the REE patterns, or REE element ratios, i.e. the terrestrial (e.g. *Microbunodon minimum*), marine (e.g. sharks), or freshwater (e.g. turtles) groups are all along the same data spread. The apparent variation is rather related to where and in which material the REE concentrations derived from. For example, the ray tooth (M4—Fig. 2A—blue-edge triangle) yielded MREE-enriched pattern in the external part of the tooth, while the internal part of root has the LREE-depleted pattern.

Stable isotope compositions

Shark tooth enameloid yielded a range of $\delta^{18}O_{PO4}$ from 19.5 to 21.9 ‰ ($n=4$) with the highest value coming from the species *Carcharoides catticus* (Additional file 4: Table S2). The single dentine analysis from the *Aralose-lachus* tooth shows a much lower value of 17.8 ‰ compared to the enameloid. The crocodilian tooth has a similar pattern in showing higher isotopic value in the enamel (19.3 ‰) than in the dentine (18.5‰). An identical trend is apparent for the terrestrial mammal teeth as well where the enamel $\delta^{18}O_{PO4}$ values are higher than those in the dentine. The upper and lower molars of *Microbunodon* yielded values of 17.4 and 16.3 ‰ in the enamel, and 15.9 and 15.4 ‰ in the dentine, respectively. In the case of the carnivore mammal (*Potamotherium* sp.), the difference between the two tooth structures is

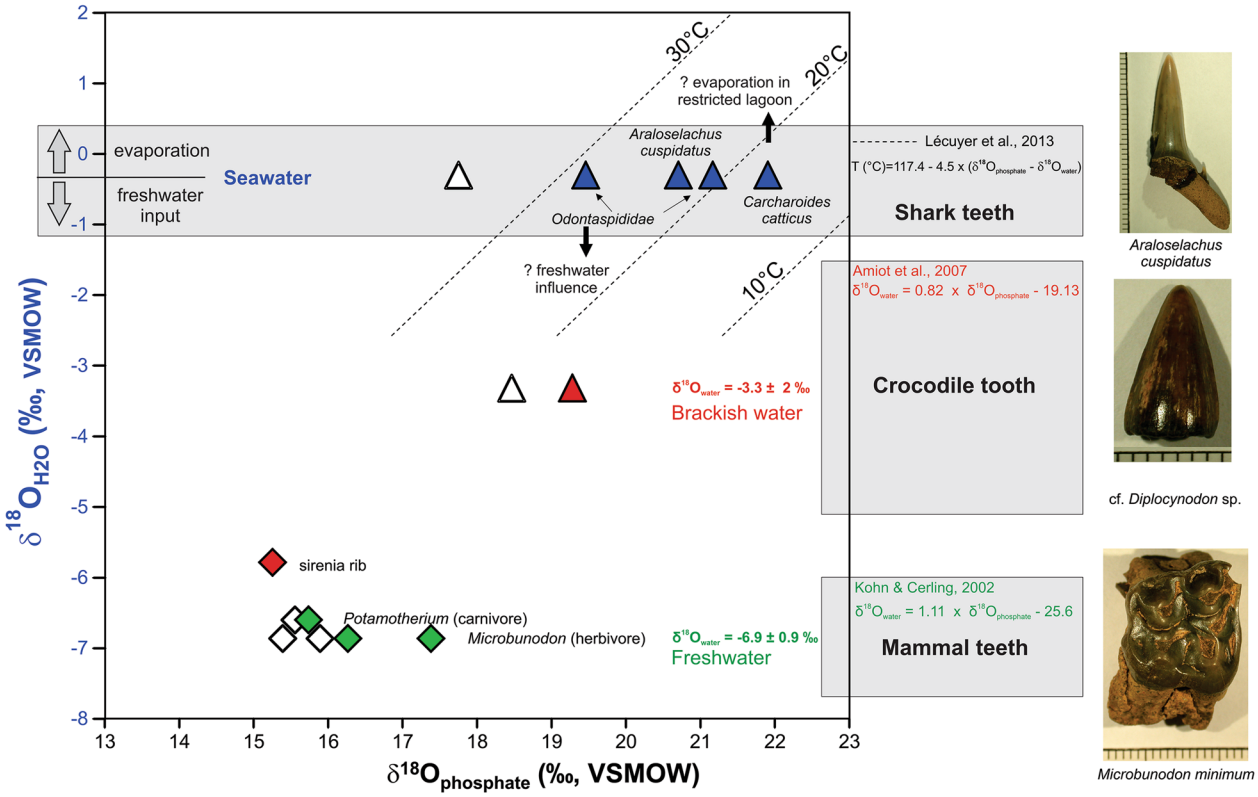

Fig. 3 Oxygen isotope composition of select vertebrate fossils from the Máriahalom site as a function of water isotopic composition. Sharks reflect seawater isotopic composition and habitat temperature (see isotherms, Lécuyer et al., 2013). It is noted that a -0.3 ‰ of seawater values was used for the Early Miocene (Lear et al., 2000), and the related marine isotope data from the shark teeth are plotted along this value. Crocodiles (cf. *Diplocynodon* sp.) most probably lived in brackish environments (Amiot et al., 2007), while mammals show the low negative $\delta^{18}O_{H2O}$ of the drinking water source (Kohn & Cerling, 2002). It is noted that the dentine and bone (sirenian) analyses have lower $\delta^{18}O_{PO4}$ compared to the enameloid/enamel that interpreted here as a sign of early diagenetic alteration in the presence of low $\delta^{18}O_{H2O}$ water

more subtle with $\delta^{18}O_{PO4}$ of 15.7 ‰ in the enamel and 15.6 ‰ in the dentine. The lowest $\delta^{18}O_{PO4}$ value comes from the seacow ribs with a value of 15.3 ‰. All the isotope data are plotted relative to environmental water isotope compositions ($\delta^{18}O_{H2O}$), which were calculated for the different taxonomic groups: fish (Lécuyer et al., 2013), crocodilians (Amiot et al., 2007), and mammals (Kohn & Cerling, 2002; Tütken, 2003) (Fig. 3).

Strontium isotope ratios and related screening methods

Three bioapatite (shark teeth) and three calcareous mollusc shells were analysed for Sr isotope ratios. Prior to this analyses the calcareous remains were tested for mineralogy, trace element, and stable isotope compositions. X-ray diffraction measurement confirmed that the calcareous remains preserved most of their original mineralogy (Table 2, Additional file 2: Figure S2), which is particularly important for the aragonitic remains (G1 and N1) as these tend to recrystalize to calcite in the diagenetic environment. The Nerineidae gastropoda is 99% of aragonite, while the *Glycymeris* bivalve besides 92% of aragonite yielded 8% of calcite. These aragonitic molluscs yielded higher $\delta^{13}C$ and $\delta^{18}O$ than the dominantly calcitic oyster shell (Table 2). The Mg/Ca and Mn/Ca ratios are higher, while the Sr/Ca ratio is lower in the oyster specimens, compared to aragonitic shells. The Fe/Ca ratio is highest in the gastropod shell (N1) and lowest in the *Glycymeris* bivalve (G1). All these data are summarized in Table 2.

The $^{87}Sr/^{86}Sr$ ratio ranges from 0.708189 to 0.708898 ($n=6$), the lowest ratio is measured in the oyster shell (O2), while the highest from the root of a shark tooth (SR2). The rest of the samples are rather confined to a relatively narrower range of 0.708364 ± 0.000029 ($n=4$), though one of the shark teeth has somewhat higher $^{87}Sr/^{86}Sr$ than the rest of the three analyses (Fig. 4). Taking the average of these three specimens and considering its 2SD error (0.708350 ± 0.00022), an age estimates of 21.4 ± 0.5 Ma can be obtained

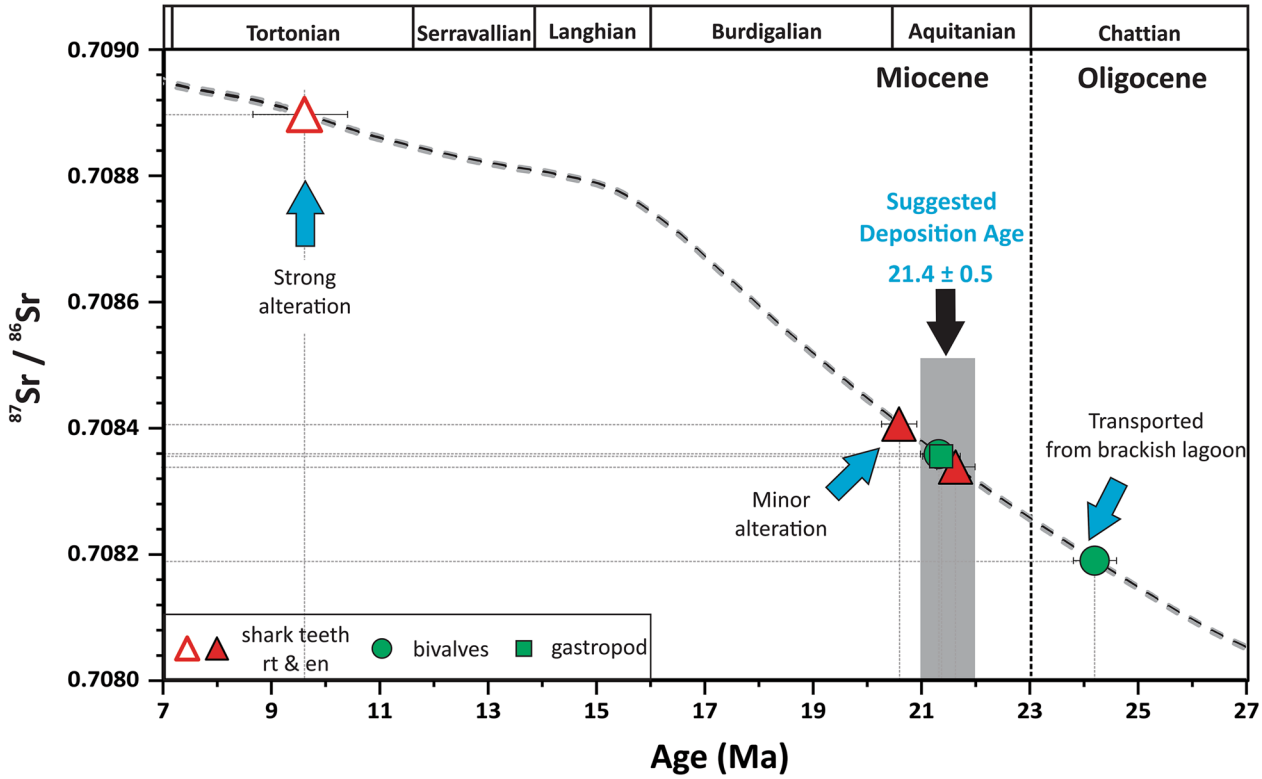

Fig. 4 Strontium isotope ratios and related ages from marine fossils recovered from the Máriahalom site. The Sr isotope evolution curve and the individual Sr isotope ages are derived from McArthur et al. (2020). The upper and lower age limits were calculated based on the 95% confidence limit of the curve and the error related to the Sr isotope analyses (external reproducibility of NIST SRM 987: 18 ppm, 2SD, $n = 14$). Bioapatite (shark teeth), aragonite, and calcite shells (molluscs) were analysed (see also Table 2). The suggested Sr isotope age of 21.4 ± 0.5 Ma for the Máriahalom site is based on the two aragonitic shells (G1 and N1), and the shark enameloid (SE1) (see Table 2) marked by a grey rectangle

(Aquitanian). However, the two extreme values would correspond to 24.2 Ma (O2—Chattian) and 9.6 Ma (SR2—Tortonian), respectively (Fig. 4). It is noted that the internal error of the individual Sr isotope analyses is smaller than that of the external error derived from repeated analyses of the NIST SRM 987 standard (18 ppm, 2SD, $n = 14$). Therefore, this higher, external error range was used to calulate the individual Sr isotope ages (Table 2).

Discussions

Rare earth element taphonomy

Rare earth elements are almost entirely of early diagenetic origin in fossil vertebrate remains (e.g. Elderfield & Pagett, 1986; Schroeter et al., 2022; Trueman, 1999, 2007; Trueman & Tuross, 2002; Trueman et al., 2006); therefore, their REE content and their distribution within the remains can be linked to depositional conditions. The REE content of the burial environment can vary based on the available REE related to local geology, sedimentology, and hydrology, while their distribution often related to redox conditions (e.g. Haley et al., 2004; Kocsis et al., 2016; Reynard et al., 1999). Therefore, remains fossilized in different environments and under different conditions (e.g. redox, terrestrial vs. marine) could inherit different REE compositions. A major implication of this is to test mixed vertebrate assemblages whether they contain fossils reworked from older and/or from different fossilization setting (e.g. Botfalvai et al, 2022; Kocsis et al., 2020, 2021; Trueman, 1999; Trueman et al., 2003). The fact that the investigated different materials from Máriahalom (e.g. bone, dentine vs enamel/enameloid) yielded similar REE distribution trends with decreasing REE concentration interiorly would partially support no, or if at all, any mixing of different REE sources, and would suggest contemporaneous REE uptake (e.g. Kohn, 2008; Trueman et al., 2011; Ullmann et al., 2020).

The relatively low REE content in the shark teeth enameloid at Máriahalom is probably explained by their inherently denser structure raised by Harrell and Pérez-Huerta (2015), Kohn (2008), and Botfalvai et al. (2022). This could relate to their substantial amounts of fluorapatite, which is composed of larger crystals, and is more stable than the carbonate hydroxylapatite found in bone tissue.

Therefore, these are less likely to recrystallize during fossilization and thus incorporate less REE. The low REE concentration in the thick mammal tooth enamel could also be related to the larger crystals, and originally lower organic content than that of dentine or bone. In case of larger remains, the internal parts within the bone cortex and teeth may not have access to pore fluid REE source, hence is their lower REE concentrations (e.g. sheltering effects of enamel for dentine). Similar, variable REE contents and different REE distribution were reported from single bones (e.g. Decrée et al., 2018).

The PAAS-normalized REE patterns and REE ratios (Fig. 3) show a trend between a middle REE-enriched and light REE-depleted patterns. Importantly, both patterns can occur in the same specimens. The LREE-depleted patterns mostly occur in the internal part of the samples, and in general, they have lower REE concentration. Therefore, these patterns are best explained by partial REE uptake driven by the limited access to REE, and by different diffusion/absorption rates along the REE series (e.g. Herwartz et al., 2011; Trueman et al., 2011) relating to their decreasing ion radii with increasing mass (i.e. lanthanide contraction). This latter process results in more effective adsorption of the LREE and MREE at the edge of the fossils during permineralization, while HREE is less likely scavenged, and it can be relatively more enriched in the interior part of the bones (e.g. Herwartz et al., 2013; Ullmann et al., 2021). Such trends have been reported from many environmental settings (e.g. Botfalvai et al., 2021, 2022; Herwartz et al., 2013; Kocsis et al., 2020; Ullmann et al., 2020). On the other hand, the MREE-enriched patterns would reflect the distribution of external REE sources related to early diagenetic pore fluids. The REE signature of natural water in the transitional zone between the marine and the terrestrial environments (such as estuaries) is highly variable, but usually is intermediate between the REE signatures of river and sea waters (Elderfield et al., 1999; Patrick et al., 2004). The LREE and MREE are preferentially adsorbed onto particle surfaces, hence in case of high sediment load in the coastal region could result in MREE-enriched patterns in vertebrate fossils such as observed in the Máriahalom assemblage (e.g. Elderfield et al., 1999; Patrick et al., 2004; Trueman et al., 2006). MREE-enriched patterns are sometimes also linked to low redox conditions and Fe redox recycling (Haley et al., 2004), and the quick sedimentation rate at the Máriahalom site may also have induced low redox conditions in the early diagenetic environment.

The similar distribution patterns of the normalized REE data from the bones and teeth of the marine, terrestrial, and freshwater animals indicate that all the investigated remains here were fossilized in similar diagenetic environments and had comparable REE uptake history. The fact that the *Microbunodon minimum* remains (both of teeth and bones) and the other measured fossils are very similar both in REE content and distributions suggest a contemporaneous fossilization for the entire vertebrate assemblage. Another implication is that even if evident mixing occurred, large-scale reworking from strata of significantly different ages can be excluded.

Ecology data

The isotope composition of teeth and bones ($\delta^{18}O_{PO4}$) of the examined taxa is closely related to environmental water isotope composition ($\delta^{18}O_{H2O}$) such as to ambient water for aquatic organisms and to consumed water for terrestrial animals (e.g. Amiot et al., 2007; Kohn & Cerling, 2002). In the case of fishes, ambient water temperature is also an important factor controlling the $\delta^{18}O_{PO4}$ values (Kolodny et al., 1983; Longinelli & Nuti, 1973).

The isotope composition of environmental water can vary a lot (e.g. Dansgaard, 1964). The average isotope composition of seawater is 0 ‰ (i.e. standardized to mean ocean water—VSMOW). However, locally, sea surface water can be more enriched in the heavy isotopes due to evaporation (positive $\delta^{18}O_{H2O}$), or it can be depleted in 18O due to freshwater input (negative $\delta^{18}O_{H2O}$). The negative $\delta^{18}O$ of freshwater is a result of successive evaporation and condensation processes of water vapour (Rayleigh fractionation), when meteoric water (i.e. precipitation) becomes more and more depleted in the heavy isotope (18O) than its original source (e.g. seawater). This depletion is further enhanced, for example, by altitude, latitude, and distance from the ocean. On the other hand, the average isotopic composition of seawater fluctuated mainly due to climatic factors such as temperature and the amount of ice in the Polar Regions in the past. Generally, for the Cenozoic the average $\delta^{18}O_{H2O}$ of seawater varied between a greenhouse and icehouse endmember values of about −1 ‰ and 0.5 ‰, respectively (e.g. Lear et al., 2000).

Two major observations can be drawn from the phosphate oxygen isotope data from Máriahalom: (1) there is a trend towards lower $\delta^{18}O_{PO4}$ values from enameloid/enamel to dentine and bone samples, and (2) there is a decrease in the enameloid/enamel isotopic values from shark teeth to the successively lower values of crocodilians and mammals (Fig. 3).

The consistent negative offset between enameloid/enamel versus dentine and the very low isotope value of the sirenia rib bone most probably reflect at least partial diagenetic overprint by low isotopic composition fluids (i.e. brackish/freshwater pore fluids). Generally, the bioapatite in dentine and bone have smaller crystallite size and higher organic content than enameloid/enamel.

These make them more prone to alteration, meaning higher susceptibility to secondary apatite formation in the pore spaces of the remains (e.g. Trueman & Tuross, 2002). In this case, some portion of the apatite would reflect the isotopic composition of the pore fluid from which it is precipitated. The fauna at the Máriahalom site clearly shows freshwater influence in the region (i.e. terrestrial mammal fossils and brackish gastropod community; Báldi, 1967; Báldi & Cságoly, 1975; Báldi, 1983; Szabó et al., 2017), and probably after deposition fresh and/or brackish pore fluid dominated the burial environment, which eventually could have enhanced the above-described diagenetic process.

The quantities of the original and secondary apatite in the vertebrate remains are difficult to assess. In case of sharks, as they replace their teeth rapidly, enameloid and dentine of the same tooth are expected to be similar in their isotopic composition. On the other hand, mammal dentine can mineralize at different stages than enamel, and in rare cases, it may remodel during the life of the animal (e.g. during healing process) (Koenigswald, 2020); hence, different $\delta^{18}O_{PO4}$ values between enamel and dentine would not be exceptional. Regarding the sirenia rib bone, the very low $\delta^{18}O_{PO4}$ value is too low for a predominantly near-shore marine mammal and the obtained value of 15.3 ‰ would indicate rather freshwater habitat (Clementz & Sewall, 2011; Tütken, 2003). However, even if trichechine sea cows (manatees) include freshwater taxa (Suarez et al., 2021), the data presented here from the bone and dentine samples are considered partially altered. Conversely, the data derived from the more resistant enameloid/enamel can be further discussed in terms of ecological conditions.

The highest $\delta^{18}O_{PO4}$ values are derived from the shark teeth (Fig. 3). The isotopic composition of fish teeth is the function of isotopic composition of environmental water and ambient temperature (Kolodny et al., 1983; Lécuyer et al., 2013; Longinelli & Nuti, 1973). When the Máriahalom shark data are plotted in the space of water and phosphate isotopic compositions with calculated isotherms (Lécuyer et al., 2013) at a Late Oligocene seawater isotopic composition (Fig. 3, −0.3 ‰, Lear et al., 2000), the observed temperature range (Fig. 3) is compatible with the inferred habitat preference of the given shark taxa (e.g. Compagno et al., 2005). As mentioned earlier, seawater isotope composition can vary due to evaporation or freshwater input especially in coastal regions. More freshwater influenced milieu would lower the $\delta^{18}O_{PO4}$ values, while habitat in evaporative lagoons / or colder, deep water could result in higher $\delta^{18}O_{PO4}$ (Fig. 3). However, variation in the isotope data among the shark teeth may not only be explained by these processes depending on where the sharks lived, but also may relate to traces of anomalous metabolic oxygen (Feng et al., 2022).

Regarding crocodilians, Amiot et al. (2007) reported a relationship between their bioapatite and ambient water isotopic composition within a precision of about ± 2 ‰: $\delta^{18}O_{H2O} = 0.82 \times \delta^{18}O_{PO4} - 19.13$. Using this correlation with the analysis of the cf. *Diplocynodon* crocodilian tooth enamel from Máriahalom an environmental water isotopic composition of −3.3 ‰ can be calculated, which indicates a brackish palaeohabitat of this animal. Most of the remains of *Diplocynodon* frequently collected from sediments deposited in freshwater environment (e.g. Buscalioni et al., 1992; Piras & Buscalioni, 2006; Delfino & Smith, 2009; Martin, 2010; Martin et al., 2014; Luján et al., 2019; Rio et al., 2019; Chroust et al., 2021 and references therein); however, *Diplocynodon* remains were also found at localities, which originated in a coastal lagoon characterized by salinity fluctuations (e.g. Monteviale, Italy: Macaluso et al., 2019; Pandolfi et al., 2016) or in normal marine conditions (Vișțea Limestone, Romania; Sabău et al., 2021). It is currently difficult to decide whether *Diplocynodon* was able to tolerate saline water or not (e.g. Brochu, 2001), but our data and the cited studies probably suggest this crocodile could have tolerated at least the brackish conditions.

Contrary to fishes and crocodilians, mammals maintain constant body temperature, and therefore, the isotope composition of their teeth reflects body fluid isotopic composition that is also influenced by the metabolism of the animal (e.g. Bryant & Froelich, 1995; Kohn & Cerling, 2002). Apart from arid-adapted mammals, most large terrestrial herbivores show a strong correlation between local water (i.e. drinking water) and bioapatite isotope compositions (e.g. $\delta^{18}O_{H2O} = 1.11 \times \delta^{18}O_{PO4} - 25.6$; Kohn & Cerling, 2002). Using only the enamel results of the *Microbunodon* teeth, environmental water of −6.9 ± 0.9 ‰ can be obtained. Therefore, the low $\delta^{18}O_{PO4}$ values in the Máriahalom mammal teeth indicate that the body fluid of these animals was influenced by this depleted water source (e.g. spring, river, lake) that was used as drinking water and/or was obtained via consumption of plants influenced by low $\delta^{18}O_{H2O}$ precipitation. Generally, *Microbunodon* lived in highly forested and marshy habitat (Boisserie, 2007; Lihoreau & Ducrocq, 2007; Tsubamoto et al., 2012), which could agree with the oxygen isotope data. Regarding the semi-aquatic carnivore mammal *Potamotherium valletoni*, the low $\delta^{18}O_{PO4}$ values (as seen for other aquatic mammals; cetacean: Roe et al., 1998; sirenian: Newsome et al., 2010) are compatible with an already inferred freshwater habitat based on depositional environments of Western European occurrences of this taxon (e.g. Savage, 1957). This is of relevance because

comprehensive phylogenies find *Potamotherium valletoni* as a stem-pinniped, and predict prolonged freshwater phases prior to marine adaptation seen in the crown group based on taphonomic data (Paterson et al., 2020). Our data lend independent support to this hypothesis, and *P. valletoni* may have not utilized the available normal marine habitats at Máriahalom.

Age of the Máriahalom site

The $^{87}Sr/^{86}Sr$ ratio of the Phanerozoic open ocean was consistent at any geological time all around the world owing to the long resident time of Sr in seawater, but the ratio varied with time as a function of gradual change in Sr influx from different Sr sources (e.g. DePaolo & Ingram, 1985; Frank, 2002; Veizer, 1989). Marine organisms, when secreting their calcareous or phosphatic hard tissues, record the actual Sr isotope ratio of the seawater; therefore, well-preserved fossils can be used to date marine sedimentary sequences via comparing the data with the Sr isotope evolution curve of the open ocean (SIS—Strontium Isotope Stratigraphy e.g. Hodell et al., 1991; Koepnick et al., 1985; McArthur et al., 2001, 2020; Veizer et al., 1997). A prerequisite is that the biominerals of the organisms are well-preserved and did not go through significant diagenetic alteration. Calcareous remains are commonly tested for original mineralogy (XRD), original shell microstructure (SEM), stable isotope, and minor/trace element compositions to ensure reliable Sr isotope ratio for age determination. Bioapatite, especially the dense crystals of tooth enameloid of fishes, has been also successfully used to date marine sequences (e.g. Harrell et al., 2016; Ingram, 1995; Kocsis et al., 2013). Nevertheless, as explained in the previous chapter, bioapatite readily uptakes REE and other trace elements during early diagenesis, and depending on the pore fluid composition in terms of Sr content, as well as Sr ratio, the fossils might be altered during this process (e.g. Martin & Scher, 2004).

Regarding the Máriahalom data, the calcareous fossils yielded original shell mineralogy. The aragonitic shells of the bivalve (G1) and gastropod (N1) have stable isotope and trace/minor element compositions that are for fully marine organisms; meanwhile, the geochemical data of the calcite oyster shell have lower $\delta^{13}C$, $\delta^{18}O$, Sr/Ca, and higher Mg/Ca ratios. This latter could indicate brackish habitat that is well known for certain oyster taxa (e.g. Kirby, 2001; Kirby et al., 1998). The relatively high Mn/Ca ratio may point towards alteration; however, in view of the brackish estuarine habitat presumed for the depositional environment of the Máriahalom site (Báldi & Cságoly, 1975), this could also be linked to in vivo incorporation. The minor presence of quartz from the XRD analyses of the oyster shell (Table 2, Additional file 2: Figure S2) may represent small grains that incorporated during shell growth in the high energy environment.

From our six Sr isotope analyses, three samples (the two aragonite shells and one shark tooth enameloid) yielded consistent Sr isotope ratios from which an average SIS age of 21.4 ± 0.5 Ma can be obtained (Aquitanian, Lower Miocene). Another shark enameloid yielded somewhat higher Sr isotope ratios (i.e. younger age of 20.6 Ma—Fig. 5), that may reflect minor alteration of its $^{87}Sr/^{86}Sr$ ratio. The sampled shark tooth root clearly reflects strong alteration with a derived false Tortonian age (which can be completely excluded due to the stratigraphical position of the site). These agree well with the earlier-mentioned observation from the REE and stable isotope studies as the more porous vertebrate materials (i.e. tooth root) were affected by more enhanced pore fluid exchange and alteration. The lowest Sr ratio comes from the calcite oyster shell corresponding to an SIS age of 24.2 Ma (Chattian, Upper Oligocene). In view of the other Sr isotope data, such old age could be explained by reworked origin of this shell from older beds; however, this would contradict with the interpretation of the REE data derived from the vertebrates. Alternatively, the lower Sr content and stable isotopic ratios could also indicate brackish conditions and, in part, freshwater Sr source that may have been influenced by somewhat older sediments that could have been exposed in the hinterland and drained into the basin (e.g. the clastic Csatka Fm—see Fig. 1—it contains Mesozoic and Eocene carbonate pebbles as well see Báldi, 1983).

The previously suggested age of the Máriahalom fauna was Egerian (Late Oligocene—Early Miocene), and due to the lack of global biostratigraphic markers, the actual Oligocene—Miocene boundary cannot be determined in the Paratethys. Despite this chronostratigraphic uncertainty of the Egerian stage, the exposed section of the Mány Member at the Máriahalom site was interpreted and reported as an Upper Oligocene succession (Báldi & Cságoly, 1975; Rabi & Botfalvai, 2008; Rabi et al., 2018; Szabó et al., 2017). Two main arguments are often brought up supporting the Oligocene age:

(1) The Máriahalom site belongs to the lower part of "Mány Formation", where the top of the Egerian stage may have been missing due to an erosional unconformity (Báldi & Cságoly, 1975; Piller et al., 2007). This is based on the brackish mollusc fauna of the site that is normally common in the lower part of the "Mány Formation", while the upper part of the member is characterized by a sub-littoral marine fauna where the brackish elements are totally absent (Báldi & Cságoly, 1975). However, more recent lithostratigraphic work considers

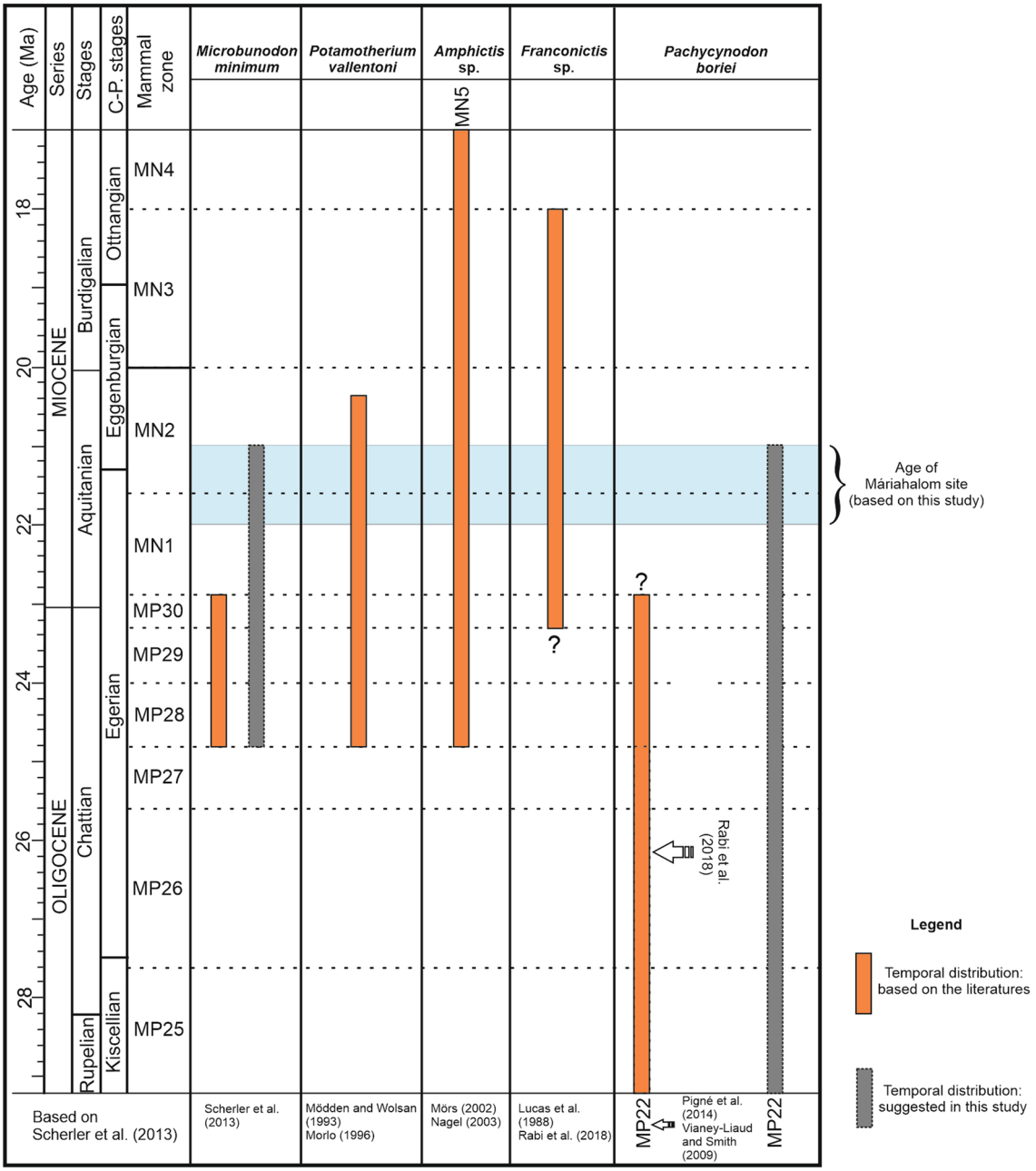

Fig. 5 Temporal range of different mammalian taxa discovered from the Máriahalom site based on the literature and the new data mentioned in this study. *C-P. stages* Central Paratethys stages, based on Petrik et al. (2014)

the "Mány Formation" as an interfingering unit of the normal marine Törökbálint Formation (Mány Member; Nagymaros et al., 2023).

(2) The anthracothere mammal *Microbunodon minimum* (Cuvier, 1822) from Máriahalom site (Rabi & Botfalvai, 2008; Rabi et al., 2018) constrains the age to the MP28–MP30 mammal zone (European Mammal Paleogene Reference Levels) of the Upper Oligocene (Late Chattian; Lihoreau et al., 2004; Mennecart, 2015; Russell et al., 1982; Scherler et al., 2013).

Based on our new Sr isotope analyses we suggest an Aquitanian age of 21.4 ± 0.5 Ma for the sediments of the Máriahalom site. Our REE analysis suggests a common diagenetic history of *Microbunodon minimum*

with that of other fossils from the locality and contemporaneous marine and terrestrial taxa. So far, the youngest occurrence of *Microbunodon minimum* has been reported from MP30 mammal level (~ 22.9 Ma see Mennecart, 2015; Scherler et al., 2013); hence, assuming that the terrestrial mammals and sharks from Máriahalom are synchronous, our data would stretch the temporal range of this taxon with at least 1–1.5 million years. This statement, however, seems to be of great importance, since the European occurrence of *Microbunodon minimum* can be dated to a restricted time interval (MP28–MP30 zones) of major faunal renewal in Europe. The MP28 marked an important immigration event in Western Europe resulting in progressive replacement of the Arvernian, hoofed mammals towards the establishment of the "classical" Agenian fauna (see details in Mennecart, 2015; Scherler et al., 2013). This transition started with MP28 and involved the appearance of *Microbunodon* in Europe. Due to its high significance in the reorganization of European ungulate communities, Scherler et al. (2013) proposed the name "*Microbunodon* event" to designate the starting datum of this important period. *Microbunodon minimum* is considered to have a short-term occurrence in Western Europe (Austria, France, Germany, and Switzerland) from MP28 to MP30 (Lihoreau et al., 2004; Scherler et al., 2013). The emergence of *M. minimum* in Europe seems to be linked to the global climatic event, named as Late Oligocene Warming (Zachos et al., 2001). The disappearance of the *Microbunodon minimum* occurred in the MP30 zone based on the Western European record (Scherler et al., 2013), which may be linked to another global climatic change, named as Mi-1 Glaciation Event. Mi-1 Glaciation Event can be characterized by decrease in temperature and humidity, and the palaeoenvironment became more mosaic like, represented by open landscapes and closed woodlands (Costeur et al., 2012; Mennecart, 2015). However, despite the comprehensive synthesis works published in the last decade, the timing and the causes of this short-term occurrence of *Microbunodon minimum* in Europe are still not well understood, and the fossil record is mainly based on remains of Western Europe. In any case, the dates of appearance and disappearance of this taxon are well-correlated with the mentioned two global climate changes, so the associated changes in vegetation can certainly provide a reasonable explanation for the brief occurrence of this animal, at least in Western Europe. The opening of the environment with less forest during the Latest Oligocene detected at the Western European localities (e.g. Becker et al., 2009; Mennecart, 2015; Mennecart et al., 2012; Scherler et al., 2013) could well have affected *M. minimum*, to have lived in a forested environment (Lihoreau & Ducrocq, 2007). Nevertheless, these environmental conditions were not uniform throughout the whole continent of Europe. Therefore, it cannot be excluded that vegetation conditions to the east or south of the Western European localities may have allowed this species to survive after the Oligocene–Miocene transition. Several tectonic events and geographical changes (e.g. Alpine orogeny) occur throughout the European Late Oligocene and Early Miocene geological history, which has created many geographical barriers (e.g. European Cainozoic Rift System or the different sub-basins of Paratethys) among different parts of Europe, where the different areas could have hosted slightly different vegetation and mammalian fauna compositions (Costeur & Legendre, 2008; Mennecart, 2015). Even between well-studied Western European localities, there are significant differences in the composition of mammal faunas during the Oligocene–Miocene transition (Costeur & Legendre, 2008; Costeur et al., 2012; Mennecart, 2015). Western European sites (especially vertebrate localities of France, Germany, and Switzerland) with their high diversity and several fossil-rich horizons provide most of the material for the establishment of the mammalian levels during the Oligocene and Miocene periods, which is understandable, since the eastern European material is less studied, and the age of the sites is often unclear (e.g. Rabi et al., 2018; Scherler et al., 2013). Our new $^{87}Sr/^{86}Sr$ data for Máriahalom mammal locality suggest that *Microbunodon minimum* may have survived till the MN 1–2 mammal zone (European Mammal Neogene Reference Levels) in the Central Paratethys region. This area was characterized by various combinations of mesophilous (zonal vegetation), riparian as well as swamp (intrazonal vegetation) vegetation types under humid subtropical climate during the Egerian (Erdei & Bruch, 2004; Hably, 1988, 1994 and references therein), which palaeoenvironment could have been a refuge area for *M. minimum*.

An alternative explanation is that the upper age limit of MP30 may not be precisely constrained (i.e. younger than ~ 22.9 Ma of Mennecart, 2015 and Scherler et al., 2013) since it is generally problematic to correlate terrestrial faunas (corresponding to temporally shorter levels) with better-dated marine faunas (temporally longer zones).

Besides *Microbunodon minimum*, four other mammalian taxa were described from Máriahalom including the semi-aquatic basal mustelid *Potamotherium valletoni*, the small-sized, terrestrial basal mustelidan *Amphictis* sp. or *Franconictis* sp., another indeterminate basal mustelidan, and the medium-sized, terrestrial basal ursoid *Pachycynodon boriei* (Rabi et al., 2018). Based on the fossil record

of *Potamotherium valletoni* reported from France, Western Germany, and Switzerland, this taxon was present in Europe between MP28 and MN2a (Mödden & Wolsan, 1993; Morlo, 1996; Mörs & von Königswald, 2000); thus, our age data (MN1–2) for the Máriahalom site do not contradict with the presence of this taxon. Both *Amphictis* and *Franconictis* survive the Oligocene–Miocene transition and they were present in Europe until MN5 and MN3, respectively (Lucas et al., 1988; Mörs, 2002; Mörs et al., 2000; Nagel, 2003). On the other hand, the *Pachycynodon boriei* described from Máriahalom is perhaps problematic, since well-dated occurrences of this taxon have so far only been reported from the Early Oligocene (MP22) from France (Peigné et al., 2014; Rabi et al., 2018; Vianey–Liaud & Schmid, 2009). Rabi et al. (2018) suggested "the *P. boriei* material from Máriahalom extends the temporal distribution of this species to the late Oligocene (MP28–30)", but in the view of our Sr isotope data this could be further extended into the earliest Miocene. It should be noted, however, that the genus *Pachycynodon* is restricted to the Oligocene (MP22), but in this case too, all the European data are from Western Europe (Peigné et al., 2014; Vianey–Liaud & Schmid, 2009).

Conclusions

The fossil vertebrate site of Máriahalom is investigated here with different geochemical approaches. The REE chemistry of the vertebrate remains points to alike early diagenetic conditions and REE source in the burial environment. Consequently, even if the fauna is mixed, significantly older reworked fossils cannot be expected. The $\delta^{18}O_{PO4}$ data analysed on shark, crocodile, and land mammal teeth reflect marine, brackish/freshwater and terrestrial habitats, and suggest freshwater preference for the stem-pinniped *Potamotherium valletoni*. The $^{87}Sr/^{86}Sr$ data derived from well-preserved calcareous marine remains and shark teeth enameloid suggest an Aquitanian age (21.4 ± 0.5 Ma) for the sediments of the Máriahalom site, that is younger than the previously reported Late Oligocene age. In the view of this new age estimate, the mammal taxa of *Microbunodon minimum* and *Pachycynodon boriei* may have survived in the Central Paratethys region after the Oligocene–Miocene boundary and was present up till the MN1–2 biostratigraphic level. In the future, with the availability of additional age data, the temporal distributions of mammalian species in East-Central Europe areas will be further determined, which would provide a better understanding of the temporal and geographic changes in the mammalian faunas of Europe.

Supplementary Information

The online version contains supplementary material available at https://doi.org/10.1186/s13358-023-00281-7.

Additional file 1: Figure S1. Specimens used for the rare earth element analyses.

Additional file 2: Figure S2. X-ray diffraction results from the calcareous remains involved in the Sr isotope analyses (N1, G1, and O2, see Table 2).

Additional file 3: Table S1. PAAS-normalized rare earth element data derived from sixteen Máriahalom vertebrates remains.

Additional file 4: Table S2. Oxygen isotope composition of the investigated vertebrate remains from the Máriahalom site.

Acknowledgements

The support of the János Bolyai Research Scholarship of the Hungarian Academy of Sciences to G.B and the ELKH-MTM-ELTE Paleo Contribution [no. 374] are much appreciated. The authors are grateful for the constructive comments of Thomas Tütken and Daniel Herwartz on an early version of the manuscript.

Author contributions

GB, LK, and MR were involved in project design; GB and LK contributed to project management; LK, GB, MR, AC, and AU were involved in data acquisition and curation; GB, AC, IF, LK, and AU performed analyses; LK and GB were responsible for primary draft of manuscript; MR, LK and GB contributed to editing and reviewing; MR, GB, and LK were responsible for funding.

Funding

Open access funding provided by University of Lausanne. This research was supported by the Hungarian National Research, Development, and Innovation Office (project NKFIH/OTKA PD 131557) to G.B.

Availability of data and materials

All of the investigated fossils are housed at the palaeontological collections of the Hungarian Natural History Museum in Budapest (NHMUS). The geochemical data are provided in the Supplementary Table files.

Declarations

Competing interests

The authors declare that they have no competing interests.

Received: 8 May 2023 Accepted: 4 July 2023
Published online: 23 August 2023

References

Amiot, R., Lécuyer, C., Escargual, G., Billon-Bruyat, J.-P., Buffetaut, E., Langlois, C., Martin, S., Martineau, F., & Mazin, J.-M. (2007). Oxygen isotope fractionation between crocodilian phosphate and water. *Palaeogeography, Palaeoclimatology, Palaeoecology, 243*, 412–420.

Anderson, P. E., Benton, M. J., Trueman, C. N., Paterson, B. A., & Cuny, G. (2007). Palaeoenvironments of vertebrates on the southern shore of Tethys: The nonmarine early cretaceous of Tunisia. *Palaeogeography, Palaeoclimatology, Palaeoecology, 243*, 118–131.

Báld, T. (1967). A Mány-Zsámbéki-Medence Felsőoligocén Makrofaunája. *Földtani Közlöny, 97*, 437–446.

Báldi, T. (1973). *Mollusc fauna of the Hungarian Upper oligocene (Egerien)*. Akadémiai Kiadó.

Báldi, T. (1983). *Magyarországi oligocén és alsómiocén formációk*. Akadémia Kiadó.

Báldi, T., & Cságoly, É. (1975). Faziostratotypus: Máriahalom sand pit. In T. Báldi & J. Senes (Eds.), *Chronostratigraphie und neostratotypen* (pp. 134–137). OM Egerien, VEDA.

Báldi, T., Less, G., & Mandic, O. (1999). Some new aspects of the lower boundary of the Egerian stage (Oligocene, chonostratigraphic scale of Paratethyan area). *Abhandlungen Der Geologischen Bundesanstalt, 56*, 653–668.

Becker, D., Bürgin, T., Oberli, U., & Scherler, L. (2009). *Diaceratherium lemanense* (Rhinocerotidae) from Eschenbach (eastern Switzerland): Systematics, palaeoecology, palaeobiogeography. *Neues Jahrbuch Für Geologie Und Paläontologie, 254*(1–2), 5–39.

Behrensmeyer, A. K. (1991). Terrestrial vertebrate accumulations. In P. A. Allison & D. E. G. Briggs (Eds.), *Taphonomy: Releasing the data locked in the fossil record* (pp. 291–335). Plenum.

Boisserie, J.-R., 2007. Family Hippopotamidae. In D.R. Prothero & S.E. Foss (Eds.), The evolution of artiodactyls (pp. 106–119). Baltimore, Maryland, Johns Hopkins University Press.

Botfalvai, G., Csiki-Sava, Z., Grigorescu, D., & Vasile, S. (2017). Taphonomical and palaeoecological investigation of the Late Cretaceous (Maastrichtian) Tuștea vertebrate assemblage (Romania; Hațeg Basin) e insights into a unique dinosaur nesting locality. *Palaeogeography, Palaeoclimatology, Palaeoecology, 468*, 228–262.

Botfalvai, G., Csiki-Sava, Z., Kocsis, L., Gáspár, A., Magyar, J., Bodor, R. E., Țabără, D., Ulyanov, A., & Makádi, L. (2021). X' marks the spot! Sedimentological, geochemical and palaeontological investigations of Late Cretaceous (Maastrichtian) vertebrate fossil localities from Vălioara Valley (Densus-Ciula Formation, Hateg Basin, Romania). *Cretaceous Research, 123*, 104781.

Botfalvai, G., Kocsis, L., Szabó, M., Király, E., & Sebe, K. (2022). Preliminary report on rare earth element taphonomy of a miocene mixed age fossil vertebrate assemblage (Pécs-Danitzpuszta, Mecsek Mts., Hungary): uptake mechanism and possible separation of palaeocommunities. *Historical Biology*. https://doi.org/10.1080/08912963.2022.2049771

Botfalvai, G., Ősi, A., & Mindszenty, A. (2015). Taphonomical and Palaeoecological investigation of the Late Cretaceous (Santonian) Iharkút vertebrate assemblage (northwestern Hungary; Bakony Mts.). *Palaeogeography, Palaeoclimatology, Palaeoecology, 417*, 379–405.

Brochu, C. A. (2001). Congruence between physiology, phylogenetics and the fossil record on crocodylian historical biogeography. In G. C. Grigg, F. Seebacher, & C. E. Franklin (Eds.), *Crocodilian biology and evolution* (pp. 9–28). Surrey Betty & Sons.

Bryant, J. D., & Froelich, P. N. (1995). A model of oxygen isotope fractionation in body water of large mammals. *Geochimica Et Cosmochimica Acta, 59*, 4523–4537.

Burke, W. H., Denison, E. R., Hetherington, A. E., Koepnick, B. R., Nelson, F. H., & Otto, B. J. (1982). Variation of seawater 87Sr/86Sr throughout Phanerozoic time. *Geology, 10*, 516–519.

Buscalioni, A. D., Sanz, J. L., & Casanovas, M. L. (1992). A new species of the eusuchian crocodile diplocynodon from the eocene of Spain. *Neues Jahrbuch Für Geologie Und Paläontologie, Abhandlungen, 187*(1), 1–29.

Chroust, M., Mazuch, M., Ivanov, M., Ekrt, B., & Luján, Á. H. (2021). First remains of Diplocynodon cf. ratelii from the early Miocene sites of Ahníkov (Most Basin, Czech Republic). *Bulletin of Geosciences, 96*(2), 123–138.

Clementz, M. T., & Sewall, O. J. (2011). Latitudinal gradients in greenhouse seawater $\delta^{18}O$: Evidence from Eocene Sirenian Tooth Enamel. *Science, 332*, 455–458.

Compagno, L. J. V., Dando, M., & Fowler, S. (2005). *Sharks of the world*. Harper Collins Publishers.

Costeur, L., & Legendre, S. (2008). Spatial and temporal variation in European Neogene large mammals diversity. *Palaeogeography, Palaeoclimatology, Palaeoecology, 261*, 127–144.

Costeur, L., Maridet, O., Peigné, S., & Heizmann, E. P. J. (2012). Palaeoecology and palaeoenvironment of the Aquitanian locality Ulm-Westtangente (MN2, Lower Freshwater Molasse, Germany). *Swiss Journal of Palaeontology, 131*, 183–199.

Dansgaard, W. (1964). Stable isotopes in precipitation. *Tellus, 16*, 436–468.

Decrée, S., Herwartz, D., Mercadier, J., Miján, I., de Buffrénil, V., Leduc, T., & Lambert, O. (2018). The post-mortem history of a bone revealed by its trace element signature: The case of a fossil whale rostrum. *Chemical Geology, 477*, 137–150.

Delfino, M., & Smith, T. (2009). A reassessment of the morphology and taxonomic status of '*Crocodylus' depressifrons* Blainville, 1855 (Crocodylia, Crocodyloidea) based on the early Eocene remains from Belgium. *Zoological Journal of the Linnean Society, 156*, 140–167.

DePaolo, D. J., & Ingram, L. B. (1985). High-resolution stratigraphy with strontium isotopes. *Science, 227*, 938–941.

Dettman, D. L., Kohn, M. J., Quade, J., Ryerson, F. J., Ojha, T. P., & Hamidullah, S. (2001). Seasonal stable isotope evidence for a strong Asian monsoon throughout the past 10.7 m.y. *Geology, 29*, 31–34.

Elderfield, H., & Pagett, R. (1986). Rare earth elements in ichthyoliths: Variations with redox conditions and depositional environment. *Science of the Total Environment, 49*, 175–197.

Elderfield, H., Upstill-Goddard, R., & Sholkovitz, E. R. (1999). The rare earth elements in rivers, estuaries, and coastal seas and their significance to the composition of ocean waters. *Geochimica Et Cosmochimica Acta, 54*, 971–991.

Erdei, B., & Bruch, A. A. (2004). A climate analysis of Late Oligocene (Egerian) macrofloras from Hungary. *Studia Botanica Hungarica, 35*, 5–23.

Feng, D., Tütken, T., Löffler, N., Tröster, G., & Pack, A. (2022). Isotopically anomalous metabolic oxygen in marine vertebrates as physiology and atmospheric proxy. *Geochimica Et Cosmochimica Acta, 328*, 85–102.

Frank, M. (2002). Radiogenic isotopes. Tracers of past ocean circulation and erosional input. *Reviews of Geophysics, 40*, 1–38.

Fricke, H. C., Clyde, W. C., & O'Neil, J. R. (1998). Intra-tooth variations in delta O-18 (PO4) of mammalian tooth enamel as a record of seasonal variations in continental climate variables. *Geochimica Et Cosmochimica Acta, 62*, 1839–1850.

Gradstein, F. M., Ogg, J. G., Schmitz, M. D., & Ogg, G. M. (2020). *A geologic time scale 2020*. Elsevier B.V.

Hably, L. (1988). Egerian fossils flora from Kesztölc, NW Hungary. *Studia Botanica Hungarica, 22*, 3–78.

Hably, L. (1994). Egerian plant fossils from Pomáz, Hungary. *Fragmenta Mineralogica Et Palaeontologica, 17*, 5–70.

Haley, B. A., Klinkhammer, G. P., & McManus, J. (2004). Rare earth elements in pore waters of marine sediments. *Geochimica Et Cosmochimica Acta, 68*(6), 1265–1279.

Harrell, T. L., Jr., & Pérez-Huerta, A. (2015). Rare earth element (REE) analysis of vertebrate fossils from the Upper Cretaceous carbonate marine formations of Western and Central Alabama, USA: Taphonomic and paleoenvironmental implications. *Palaios, 30*, 514–528.

Harrell, T. L., Pérez-Huerta, A., & Phillips, G. (2016). Strontium isotope age-dating of fossil shark tooth enameloid from the Upper Cretaceous Strata of Alabama and Mississippi, USA. *Cretaceous Research, 62*, 1–12.

Harzhauser, M., & Piller, W. E. (2007). Benchmark data of a changing sea—palaeogeography, palaeobiogeography and events in the Central Paratethys during the Miocene. *Palaeogeography, Palaeoclimatology, Palaeoecology, 253*, 8–31.

Herwartz, D., Tütken, T., Jochum, K. P., & Sander, P. M. (2013). Rare earth element systematics of fossil bone revealed by LA-ICPMS analysis. *Geochimica Et Cosmochimica Acta, 103*, 161–183.

Herwartz, D., Tütken, T., Münker, C., Jochum, K. P., Stoll, B., & Sander, P. M. (2011). Timescales and mechanisms of REE and Hf uptake in fossil bones. *Geochimica Et Cosmochimica Acta, 75*, 82–105.

Hodell, D. L., Mueller, A. P., & Garrido, R. J. (1991). Variations in the strontium isotopic composition of seawater during the Neogene. *Geology, 19*, 24–27.

Ingram, B. L. (1995). High-resolution dating of deep-sea clays using Sr isotopes in fossil fish teeth. *Earth and Planetary Science Letters, 134*, 545–555.

Janssen, A. W. (1982). Late Oligocene molluscs from a sand-pit near Máriahalom (Hungary). A preliminary study. *Annales Universitatis Scientiarum Sectio Geologica, 14*, 109–150.

Kázmér, M., Dunkl, I., Frisch, W., Kuhlemann, J., & Ozsvárt, P. (2003). The Paleogene forearc basin of the Eastern Alps and Western Carpatians: Subduction erosion and basin evolution. *Journal of the Geological Society, 160*, 413–428.

Keenan, S. W., & Engel, A. S. (2017). Early diagenesis and recrystallization of bones. *Geochimica Et Cosmochimica Acta, 196*, 209–223.

Kirby, M. X. (2001). Differences in growth rate and environment between tertiary and quaternary Crassostrea oysters. *Paleobiology, 27*(1), 84–103.

Kirby, M. X., Soniat, T. M., & Spero, H. J. (1998). Stable isotope sclerochronology of pleistocene and recent oyster shells (*Crassostrea virginica*). *Palaios, 13*, 560–569.

Kocsis, L., Botfalvai, G., Qamarina, Q., Razak, H., Király, E., Lugli, F., Wings, F., Lambertz, M., Raven, H., Briguglio, A., & Rabi, M. (2020). Geochemical

analyses suggest stratigraphic origin and late Miocene age of reworked vertebrate remains from Penanjong Beach in Brunei Darussalam (Borneo). *Historical Biology*. https://doi.org/10.1080/08912963.2020.1819999

Kocsis, L., Gheerbrant, E., Mouflih, M., Cappetta, H., Ulianov, A., Chiaradia, M., & Bardet, N. (2016). Gradual changes in upwelled seawater conditions (redox, pH) from the late cretaceous through early paleogene at the northwest coast of Africa: Negative Ce anomaly trend recorded in fossil bio-apatite. *Chemical Geology, 421*, 44–54.

Kocsis, L., Ounis, A., Chaabani, F., & Salah, N. M. (2013). Paleoenvironmental conditions and strontium isotope stratigraphy in the Paleogene Gafsa Basin (Tunisia) deduced from geochemical analyses of phosphatic fossils. *International Journal of Earth Sciences, 102*, 1111–1129.

Kocsis, L., Ozsvárt, P., Becker, D., Ziegler, R., Scherler, L., & Codrea, V. (2014). Orogeny forced terrestrial climate variation during the late Eocene-early oligocene in Europe. *Geology, 42*, 727–730.

Kocsis, L., Trueman, C. N., & Palmer, M. R. (2010). Protracted diagenetic alteration of REE contents in fossil bioapatites: Direct evidence from Lu–Hf isotope systematics. *Geochimica Et Cosmochimica Acta, 74*, 6077–6092.

Kocsis, L., Ulianov, A., Mouflih, M., Khaldoune, F., & Gheerbrandt, E. (2021). Geochemical investigation of the taphonomy, stratigraphy, and palaeoecology of the mammals from the Ouled Abdoun Basin (Paleocene-Eocene of Morocco). *Palaeogeography, Palaeoclimatology, Palaeoecology, 577*, 110523.

Koenigswald, W. v., (2020). Construction and wear of mammalian teeth in terms of heterochrony. In T. Martin & W. v. Koenigswald (Eds.), Mammalian Teeth – Form and Function (pp. 171–186). München, Verlag Dr. Friedrich Pfeil. - https://doi.org/10.23788/mammteeth.09

Koepnick, R. B., Burke, H. W., Denison, E. R., Hetherington, A. E., Nelson, F. H., Otto, J. B., & Waite, E. L. (1985). Construction of the seawater 87Sr/86Sr curve for the Cenozoic and cretaceous: Supporting data. *Chemical Geology, 58*, 55–81.

Kohn, M. J. (2008). Models of diffusion-limited uptake of trace elements in fossils and rates of fossilization. *Geochimica Et Cosmochimica Acta, 72*, 3758–3770.

Kohn, J. M., & Cerling, E. T. (2002). Stable isotope compositions of biological apatite. In J. M. Kohn, J. Rakovan, & J. M. Hughes (Eds.), *Phosphates: Geochemical, geobiological, and materials importance. Review in mineralogy and geochemistry 48* (pp. 455–488). The Mineralogical Society of America.

Kohn, J. M., & Moses, J. R. (2012). Trace element diffusivities in bone rule out simple diffusive uptake during fossilization but explain in vivo uptake and release. *Proceedings of the National Academy of Sciences, 110*(2), 419–424.

Kolodny, Y., Luz, B., & Navon, O. (1983). Oxygen isotope variations in phosphate of biogenic apatites, I. Fish bone apatite-rechecking the rules of the game. *Earth and Planetary Science Letters, 64*, 398–404.

Korpás, L. (1981). A Dunántúli-középhegység oligocén—alsó-miocén képződményei. (Oligocene—lower Miocene formations of the transdanubian central mountains in Hungary). *Magyar Állami Földtani Intézet Évkönyve, 64*(1), 1–80.

Kowal-Linka, M., Jochum, K. P., & Surmik, D. (2013). LA-ICP-MS analysis of rare earth elements in marine reptile bones from the middle Triassic bonebed (Upper Silesia, S Poland): Impact of long-lasting diagenesis, and factors controlling the uptake. *Chemical Geology, 363*, 213–228.

Lear, H. C., Elderfield, P., & Wilson, P. A. (2000). Cenozoic deep-sea temperatures and global ice volumes from Mg/Ca in benthic foraminiferal calcite. *Science, 287*, 269–272.

Lécuyer, C., Amiot, R., Touzeau, A., & Trotter, J. (2013). Calibration of the phosphate $\delta^{18}O$ thermometer with carbonate–water oxygen isotope fractionation equations. *Chemical Geology, 347*, 217–226.

Less, Gy., Frijia, G., Filipescu, S., Holcová, K., Madic, O., & Sztanó, O. (2015). New Sr-isotope stratigraphy (SIS) age-data from the Central Paratethys. 2nd International congress on Stratigraphy. Abstract volume, p. 223

Lihoreau, F., Blondel, C., Barry, J., & Brunet, M. (2004). A new species of the genus *Microbunodon* (anthtacothere, Artiodactyla) from the Miocene of Pakistan: Genus revision, phylogenetic relationships and palaeobiogeography. *Zoologica Scripta, 33*, 97–115.

Lihoreau, F., & Ducrocq, S. (2007). Family anthtacothere. In D. R. Prothero & S. E. Foss (Eds.), *The evolution of artiodactyls* (pp. 89–105). Johns Hopkins University Press.

Longinelli, A. (1984). Oxygen isotopes in mammal bone phosphate: A new tool for palaeoclimatological and palaeoenvironmental research? *Geochimica Et Cosmochimica Acta, 48*, 385–390.

Longinelli, A., & Nuti, S. (1973). Oxygen isotope measurements from fish teeth and bones. *Earth and Planetary Science Letters, 20*, 373–376.

Lucas, G. S., Emry, R. J., & Tleuberdina, P. A. (1988). Franconictis (Mammalian: Carnivora) from the late oligocene of eastern Kazakstan. *Proceedings of the Biological Society of Washington, 111*(3), 504–510.

Lujan, A. H., Chroust, M., Cernansky, A., Fortuny, J., Mazuch, M., & Ivanov, M. (2019). First record of *Diplocynodon ratelii* pomel, 1847 from the early Miocene site of Tušimice (Most Basin, Northwest Bohemia, Czech Republic). *Comptes Rendus Palevol, 18*, 877–889.

Macaluso, L., Martin, J. E., Del Favero, L., & Delfino, M. (2019). Revision of the crocodilians from the Oligocene of Monteviale, Italy, and the diversity of European eusuchians across the Eocene-Oligocene boundary. *Journal of Vertebrate Paleontology*. https://doi.org/10.1080/02724634.2019.1601098

Makarewicz, C. A., & Pederzani, S. (2017). Oxygen ($\delta^{18}O$) and carbon ($\delta^{13}C$) isotopic distinction in sequentially sampled tooth enamel of co-localized wild and domesticated caprines: Complications to establishing seasonality and mobility in herbivores. *Palaeogeography, Palaeoclimatology, Palaeoecology, 485*, 1–15.

Martin, J. E. (2010). A new species of Diplocynodon (Crocodilia, Alligatoroidea) from the Late Eocene of the Massif Central, France, and the evolution of the genus in the climatic context of the Late Palaeogene. *Geological Magazine, 147*(4), 596–610.

Martin, E. E., & Scher, H. D. (2004). Preservation of seawater Sr and Nd isotopes in fossil fish teeth: Bad news and good news. *Earth Planetary Science Letter, 220*, 25–39.

Martin, J. E., Smith, T., De Broin, F. L., De Escuillie, F., & Delfino, M. (2014). Late Paleocene eusuchian remains from Mont de Berru, France and the origin of the alligatoroid *Diplocynodon*. *Zoological Journal of the Linnean Society, 172*(4), 867–891.

McArthur, J. M., Howarth, R. J., & Bailey, T. R. (2001). Strontium isotope stratigraphy: LOWESS version 3: Best fit to the marine Sr-isotope curve for 0–509 Ma and accompanying look-up table for deriving numerical age. *Journal of Geology, 109*, 155–170.

McArthur, J. M., Howarth, R. J., Shields, G. A., & Zhou, Y. (2020). Strontium isotope stratigraphy, Chapter 7. In F. M. Gradstein, J. G. Ogg, M. D. Schmitz, & G. M. Ogg (Eds.), *A geologic time scale* (pp. 211–238). Elsevier B.V.

Mennecart, B. (2015). The European ruminants during the "*Microbunodon* Event" (MP28, Latest Oligocene): Impact of climate changes and faunal event on the ruminant evolution. *PlosOne, 10*(2), e0116830. https://doi.org/10.1371/journal.pone.0116830

Mennecart, B., Scherler, L., Hiard, F., Becker, D., & Berger, J.-P. (2012). Large mammals from Rickenbach (Switzerland, reference locality MP29, Late Oligocene): Biostratigraphic and palaeoenvironmental implications. *Swiss Journal of Palaeontology, 131*, 161–181.

Millard, A. R., & Hedges, R. E. M. (1996). A diffusion–adsorption model of uranium uptake by archaeological bone. *Geochimica Et Cosmochimica Acta, 60*, 2139–2152.

Miller, K. G., Browning, J. V., Schmelz, W. J., Kopp, R. E., Mountain, G. S., & Wright, J. D. (2020). Cenozoic sea-level and cryospheric evolution from deep-sea geochemical and continental margin records. *Science Advances, 6*, eaaz1346.

Mödden, C., & Wolsan, M. (1993). Potamotherium valletoni (Mammalia: Carnivora) aus dem Untermiozän von Wiesbaden-Amöneburg im Mainzer Becken. *Mainzer Naturwissenschaftlicher Archiv, 31*, 215–221.

Morlo, M. (1996). Carnivoren aus dem Unter-Miozän des Mainzer Beckens (2. Mustelida, Pinnipedia, Feliformia, Palaeogale). *Senckenbergiana Lethaea, 76*, 193–249.

Mörs, T. (2002). Biostratigraphy and paleoecology of continental tertiary vertebrate faunas in the lower Rhine embayment (NW-Germany). *Netherlands Journal of Geosciences, 81*(2), 177–183.

Mörs, T., von der Hocht, F., & Wutzler, B. (2000). Die ersteWirbeltierfauna aus der miozänen Braunkohle der Niederrheinischen Bucht (Ville-Schichten, Tagebau Hambach). *Paläontologische Zeitschrift, 74*(1/2), 145–170.

Mörs, T., & von Königswald, W. (2000). *Potamotherium valletoni* (Carnivora, Mammalia) aus dem Oberoligozän von Enspel im Westerwald. *Senckenbergiana Lethaea, 80*(1), 257–273.

Nagel, D. (2003). Carnivora from the middle Miocene hominoid locality of Çandir (Turkey). *Courier Forschungsinstitut Senckenberg, 240*, 113–131.
Nagymarosy, A. (2012). Paratethys evolution and its consequences for the Paleogene-neogene Chronostratigrapic framework. In J. Haas (Ed.), *Geology of Hungary* (pp. 81–99). Springer.
Nagymarosy, A., & Gyalog, L. (1997). Mány formation. In G. Császár (Ed.), *Basic litostratigraphic units of Hungary* (pp. 14–15). The Geological Institute of Hungary.
Nagymarosy, A., Sztanó, O., Fodor, L., & Selmeczi, I., (2023). Törökbálinti Formáció. In Babinszki et al. (Eds.), Magyarország litosztratigráfiai egységeinek leírása II. Kainozoos képződmények. (Lithostratigraphic units of Hungary II. – Cenozoic) (pp. 40), Budapest, SZTFH.
Newsome, S. D., Clementz, M. T., & Koch, P. L. (2010). Using stable isotope biogeochemistry to study marine mammal ecology. *Marine Mammal Science, 26*, 509–572.
O'Neil, J. R., Roe, L. J., Reinhard, E., & Blake, R. E. (1994). A rapid and precise method of oxygen isotope analysis of biogenic phosphate. *Israel Journal of Earth Sciences, 43*, 203–212.
Pandolfi, L., Carnevale, G., Costeur, L., Del Favero, L., Fornasiero, M., Ghezzo, E., Maiorino, L., Mietto, P., Piras, P., Rook, L., Sansalone, G., & Kotsakis, T. (2016). Reassessing the earliest Oligocene vertebrate assemblage of Monteviale (Vicenza, Italy). *Journal of Systematic Palaeontology, 15*(2), 83–127.
Paterson, R. S., Rybczynski, N., Kohno, N., & Maddin, H. C. (2020). A total evidence phylogenetic analysis of pinniped phylogeny and the possibility of parallel evolution within a monophyletic framework. *Frontiers in Ecology and Evolution, 7*, 457. https://doi.org/10.3389/fevo.2019.00457
Patrick, D., Martin, J. E., Parris, D. C., & Grandstaff, D. E. (2004). Paleoenvironmental interpretations of rare earth element signatures in mosasaurs (reptilia) from the upper Cretaceous Pierre Shale, central South Dakota, USA. *Palaeogeography, Palaeoclimatology, Palaeoecology, 212*, 277–294.
Peigné, S., Vianey-Liaud, M., Pélissié, T., & Sigé, B. (2014). Valbro: Un nouveau site à vertébrés de l'Oligocène inférieur (MP22) de France (Quercy). I—Contexte géologique; mammalia: Rodentia, Hyaenodontida. *Carnivora. Annales De Paléontologie, 100*, 1–45.
Petrik, A., Beke, B., & Fodor, L. (2014). Combined analysis of faults and deformation bands reveals the Cenozoic structural evolution of the southern Bükk foreland (Hungary). *Tectonophysics, 633*, 43–62.
Piller, W. E., Harzhauser, M., & Mandic, O. (2007). Miocene Central Paratethys stratigraphy—current status and future directions. *Stratigraphy, 4*, 151–168.
Piras, P., & Buscalioni, A. D. (2006). Diplocynodon muelleri comb. nov., an oligocene diplocynodontine alligatoroid from Catalonia (Ebro Basin, Lleida province, Spain). *Journal of Vertebrate Paleontology, 26*, 608–620.
Popov, S. V., Rögl, F., Rozanov, A. Y., Steininger, F. F., Shcherba, I. G., & Kovác, M. (2004). Lithological-paleogeographic maps of Paratethys, 10 maps late Eocene to Pliocene. *Courier Forschungsinstitut Senckenberg, 250*, 1–46.
Rabi, M., Bastl, K., Botfalvai, G., Evanics, Z., & Peigné, S. (2018). A new carnivoran fauna from the late Oligocene of Hungary. *Palaeobiodiversity and Palaeoenvironments, 98*, 509–521.
Rabi, M., & Botfalvai, G. (2008). A preliminary report of the late Oligocene vertebrae fauna from Máriahalom, Hungary. *Hantkenia, 6*, 177–185.
Reynard, B., Lécuyer, C., & Grandjean, P. (1999). Crystal–chemical controls on rare earth element concentrations in fossil biogenic apatites and implications for palaeoenvironmental reconstructions. *Chemical Geology, 155*, 233–241.
Rio, J. P., Mannion, P. D., Tschopp, E., Martin, J. E., & Delfino, M. (2019). Reappraisal of the morphology and phylogenetic relationships of the alligatoroid crocodylian *Diplocynodon hantoniensis* from the late Eocene of the United Kingdom. *Zoological Journal of the Linnean Society, 188*(2), 579–629.
Roe, L. J., Thewissen, J. G. M., Quade, J., O'Neil, J. R., Bajpai, S., Sahmi, A., & Hussain, S. T. (1998). Isotopic approaches to understanding the terrestrial-to-marine transition of the earliest cetaceans. In J. G. M. Thewissen (Ed.), *The emergence of whales* (pp. 399–422). Plenum Press.
Rögl, F. (1998). Paleogeographic consideration for Mediterranean and Paratethys seaways (Oligocene to Miocene). *Annalen Des Naturhistorischen Museums in Wien, 99A*, 279–310.
Russell, D. E., Hartenberger, J., Pomerol, C., Sen, S., Schmidt-Kittler, N., & Vianey-Liaud, M. (1982). *Mammals and stratigraphy: The paleogene of Europe* (pp. 1–77). Palaeovertebrata, Mémoir extraordinaire.
Sabău, I., Venczel, M., Codrea, V. A., & Bordeianu, M. (2021). Diplocynodon: A salt water Eocene crocodile from Transylvania? *North-Western Journal of Zoology, 17*(1), 117–121.
Savage, R. J. G. (1957). The anatomy of *Potamotherium* an Oligocene latrine. *Proceedings of the Zoological Society of London, 129*, 151–244.
Scherler, L., Mennecart, B., Hiard, F., & Becker, D. (2013). Evolution of terrestrial hoofed-mammals during the Oligocene-Miocene transition in Europe. *Swiss Journal of Geosciences, 106*, 349–369.
Schroeter, E. R., Ullmann, P. V., Macauley, K., Ash, R. D., Zheng, W., Schweitzer, M. H., & Lacovara, K. J. (2022). Soft-tissue, rare earth element, and molecular analyses of *Dreadnoughtus schrani*, an exceptionally complete titanosaur from Argentina. *Biology, 11*, 1158. https://doi.org/10.3390/biology11081158
Spötl, C., & Vennemann, T. W. (2003). Continuous-flow IRMS analysis of carbonate minerals. *Rapid Communications of Mass Spectrometry, 17*, 1004–1006.
Suarez, C., Gelfo, J. N., Moreno-Bernal, J. W., & Velez-Juarbe, J. (2021). An early Miocene manatee from Colombia and the initial Sirenian invasion of freshwater ecosystems. *Journal of South American Earth Sciences., 109*, 103277. https://doi.org/10.1016/j.jsames.2021.103277
Szabó, M., Botfalvai, G., Kocsis, L., Carnevale, G., Sztanó, O., Evanics, Z., & Rabi, M. (2017). Upper Oligocene marine fishes from near-shore deposits of the Central Paratethys (Máriahalom, Hungary). *Palaeobiodiversity and Palaeoenvironments, 97*(4), 747–771.
Szederkényi, T., Kovács, S., Haas, J., & Nagymarosy, A. (2012). *Geology and history of evolution of the ALCAPA Mega-Unit*. Springer.
Sztanó, O., Magyari, Á., & Nagymarosy, A. (1998). High-resolution stratigraphy in the Esztergom Basin, northeastern Transdanubia, Hungary: II. Oligocene sequences and their interpretation. *Földtani Közlöny, 128*, 455–486.
Tari, G., Báldi, T., & Báldi-Beke, M. (1993). Paleogene retroarc flexural basin beneath the neogene pannonian Basin: a geodynamic model. *Tectonophysics, 226*, 433–455.
Telegdi-Roth, K. (1927). Spuren einer infraoligozanen denudation am nordwestlichen range des Transdanubischen Mittelgebirge. *Földtani Közlöny, 57*, 117–128.
Trueman, C. N. (1999). Rare earth element geochemistry and taphonomy of terrestrial vertebrate assemblages. *Palaios, 14*, 555e568. https://doi.org/10.2307/3515313
Trueman, C. N. (2007). Trace element geochemistry of bonebeds. Chapter 7. In R. R. Rogers, D. A. Eberth, & A. R. Fiorillo (Eds.), *Bonebeds: Genesis, analysis and paleobiological significance* (pp. 397–435). University of Chicago Press.
Trueman, C. N., Behrensmeyer, A. K., Potts, R., & Tuross, N. (2006). High-resolution records of location and stratigraphic provenance from the rare earth element composition of fossil bones. *Geochimica Et Cosmochimica Acta, 70*, 4343–4355.
Trueman, C. N., Behrensmeyer, A. K., Tuross, N., & Weiner, S. (2004). Mineralogical and compositional changes in bones exposed on soil surfaces in Amboseli National Park, Kenya: Diagenetic mechanisms and the role of sediment pore fluids. *Journal of Archaeological Science, 31*, 721–739.
Trueman, C. N., Benton, M. J., & Palmer, M. R. (2003). Geochemical taphonomy of shallow marine vertebrate assemblages. *Palaeogeography, Palaeoclimatology, Palaeoecology, 197*, 151–169.
Trueman, C. N., Kocsis, L., Palmer, M. R., & Dewdney, C. (2011). Fractionation of rare earth elements within bone mineral: A natural cation exchange system. *Palaeogeography, Palaeoclimatology, Palaeoecology, 310*, 124–132.
Trueman, C. N., & Tuross, N. (2002). Trace elements in recent and fossil bone apatite. In J. M. Kohn, J. Rakovan, & J. M. Hughes (Eds.), *Phosphates: Geochemical, geobiological, and materials importance. Review in mineralogy and geochemistry 48* (pp. 489–521). The Mineralogical Society of America.
Tsubamoto, T., Thaung-Htike, Zin-Maung-Maung-Thein, Egi, N., Nishioka, Y., Maung-Maung, & Takai M., (2012). New data on the Neogene anthracotheres (Mammalia Artiodactyla) from central Myanmar. *Journal of Vertebrate Paleontology, 32(4)*, 956–964. https://doi.org/10.1080/02724634.2012.670176
Tütken, T. (2003). *Die Bedeutung der Knochenfrühdiagenese für die Erhaltungsfähigkeitin vivo erworbener Element- und Isotopen zusammensetzungen in fossilen Knochen*. (Ph.D.-thesis). Naturwissenschaften der Geowissenschaftlichen Fakultätder Eberhard-Karls-Universität Tübingen, Germany.

Tütken, T., Kaiser, T. M., Vennemann, T., & Merceron, G. (2013). Opportunistic feeding Strategy for the earliest old world hypsodont equids: evidence from stable isotope and dental wear proxies. *PlosOne, 8*, e74463. https://doi.org/10.1371/journal.pone.0074463

Tütken, T., Vennemann, T. W., Janz, H., & Heimann, E. P. J. (2006). Palaeoenvironment and palaeoclimate of the Middle Miocene lake in the Steinheim basin, SW Germany: A reconstruction from C, O, and Sr isotopes of fossil remains. *Palaeogeography, Palaeoclimatology, Palaeoecology, 241*, 457–491.

Ullmann, P. V., Grandstaff, D. E., Ash, R. D., & Lacovara, K. J. (2020). Geochemical taphonomy of the Standing Rock Hadrosaur Site: Exploring links between rare earth elements and cellular and soft tissue preservation. *Geochimica Et Cosmochimica Acta, 269*, 223–237.

Ullmann, P. V., Macauley, K., Ash, R. D., Shoup, B., & Scannella, J. B. (2021). Taphonomic and diagenetic pathways to protein preservation, part I: The case of Tyrannosaurus rex specimen MOR 1125. *Biology, 10*, 1193.

Veizer, J. (1989). Strontium isotopes in seawater through time. *Annual Review of Earth and Planetary Sciences, 17*, 141–167.

Veizer, J., Buhl, D., Diener, A., Ebneth, S., Podlaha, O. G., Bruckschen, P., Jasper, T., Korte, C., Schaaf, M., Ala, D., & Azmy, K. (1997). Strontium isotope stratigraphy: Potential resolution and event correlation. *Palaeogeography, Palaeoclimatology, Palaeoecology, 132*, 65–77.

Vennemann, T. W., Fricke, H. C., Blake, R. E., O'Neil, J. R., & Colman, A. (2002). Oxygen isotope analyses of phosphates: A comparison of techniques for analysis of Ag_3PO_4. *Chemical Geology, 185*, 321–336.

Vianey-Liaud, M., & Schmid, B. (2009). Diversité, datation et paléoenvironnement de la faune de mammifères oligocène de Cavalé (Quercy, SO France): Contribution de l'analyse morphométrique des Theridomyinae (Mammalia, Rodentia). *Geodiversitas, 31*(4), 909–941.

Zachos, J., Pagani, M., Sloan, L., Thomas, E., & Billups, K. (2001). Trends, rhythms, and aberrations in global climate 65 Ma to Present. *Science, 292*, 686–693.

Publisher's Note